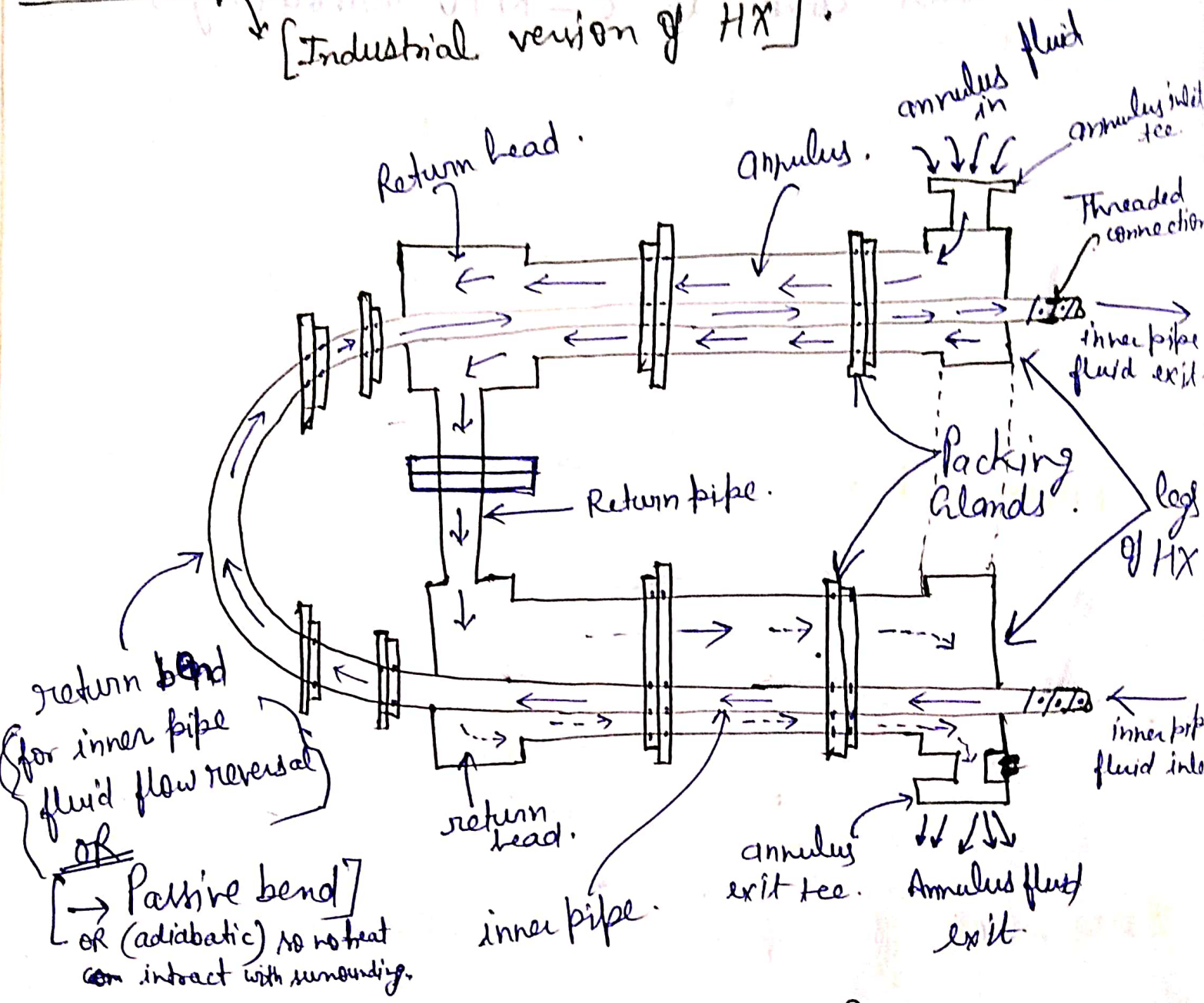


Counter-flow double pipe Heat exchanger

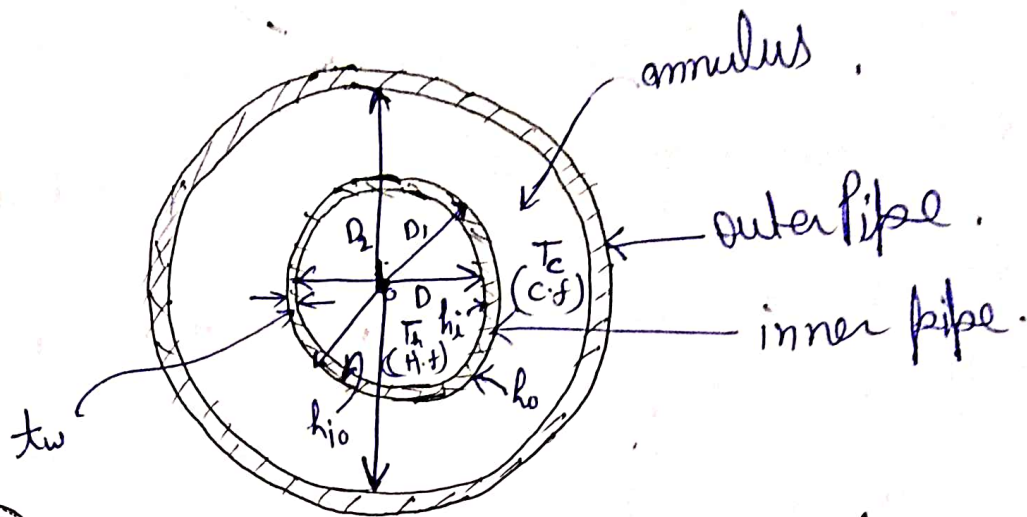
[Industrial version of HX]



It is also called Hair-Pin HX.

Return band → It is used for flow reversal, it is also called passive bend.

Mathematical calculations pertaining to Hair-Lin(m)



① Film coeff pertaining to HX →

Let D , D_1 & D_2 indicates the inside dia of inner pipe, outside dia of inner pipe and inside dia of outer pipe respectively.

t_w → thickness of inner pipe.

Let assumed that H.F at inner pipe and C.F. at annulus.

T_h & T_c indicate hot and cold fluid temp.

h_i → film coefficient of inner pipe fluid based on inner surface of inner pipe.

h_o → film coeff. of annulus fluid based on outer surface of the inner pipe.

h_{io} → film coeff. of inner pipe fluid based on outer surface of inner pipe.

Calculation for " h_i ": —

$$Re = \frac{U D \rho_{fh}}{\mu_{fh}} = \frac{D \cdot (U \rho_{fh})}{\mu_{fh}}$$

where: $U \rightarrow$ mean velo of inner pipe fluid and ~~the~~ G_h

thermo physical property (ρ_{fh} & μ_{fh}) ~~property~~

$$T_{bh} = \frac{T_{hi} + T_{he}}{2}$$

$$Re = \frac{D G_h}{\mu_{fh}} \quad \text{--- (1)}$$

$G_h \rightarrow$ mass velocity of inner pipe fluid.

$$G_h = U \rho_{fh} \quad (\text{kg/m}^2\text{-s})$$

if $Re_D \leq 2100$ & $Re_D \geq 100$

i.e. $100 \leq Re_D \leq 2100$ The flow is streamline or Laminar flow.

& the film coeffⁿ relation is given by the Sieder and Tate.

$$Nu_i = \frac{h_i D}{k_{fh}} = 1.86 \left[\left(\frac{D G_h}{\mu_{fh}} \right) \left(\frac{\mu_{fh} \rho_{fh}}{k_{fh}} \right) \left(\frac{D}{L} \right) \right]^{1/3} \times \left(\frac{\mu_{fh}}{\mu_{fhw}} \right)^{0.14} \quad \text{--- (2)}$$

where $\rightarrow L = 2 L_e$ ~~required~~

$\left(\frac{\mu_{fh}}{\mu_{fhw}} \right) \rightarrow$ the abs viscosity of inner pipe fluid pertaining to Bulk mean temp^r and wall temp^r of inner pipe.

$\frac{\mu_{fh}}{\mu_{fhw}}$ is called viscosity correction factor.

The above correlation has a mean S.D. $\pm 12\%$

* if $Re_D > 10000$ and $L/D > 60$ and $0.7 < Pr_f < 16700$ for Turbulent flow.

Sieder and Tate relation

$$Nu_i = \frac{h_i D}{k_{f,h}} = 0.027 \left(\frac{DG_{f,h}}{\mu_{f,h}} \right)^{0.8} \left(\frac{\mu_{f,h} C_{p,f,h}}{k_{f,h}} \right)^{1/3} \left(\frac{\mu_{f,h}}{\mu_{f,w}} \right)^{0.14}$$

The above relation is accurate within $\pm 15\%$ and $\pm 10\%$ max std deviation of $+15\%$ and -10% .

To calculate h_{i0} the following relation is used —

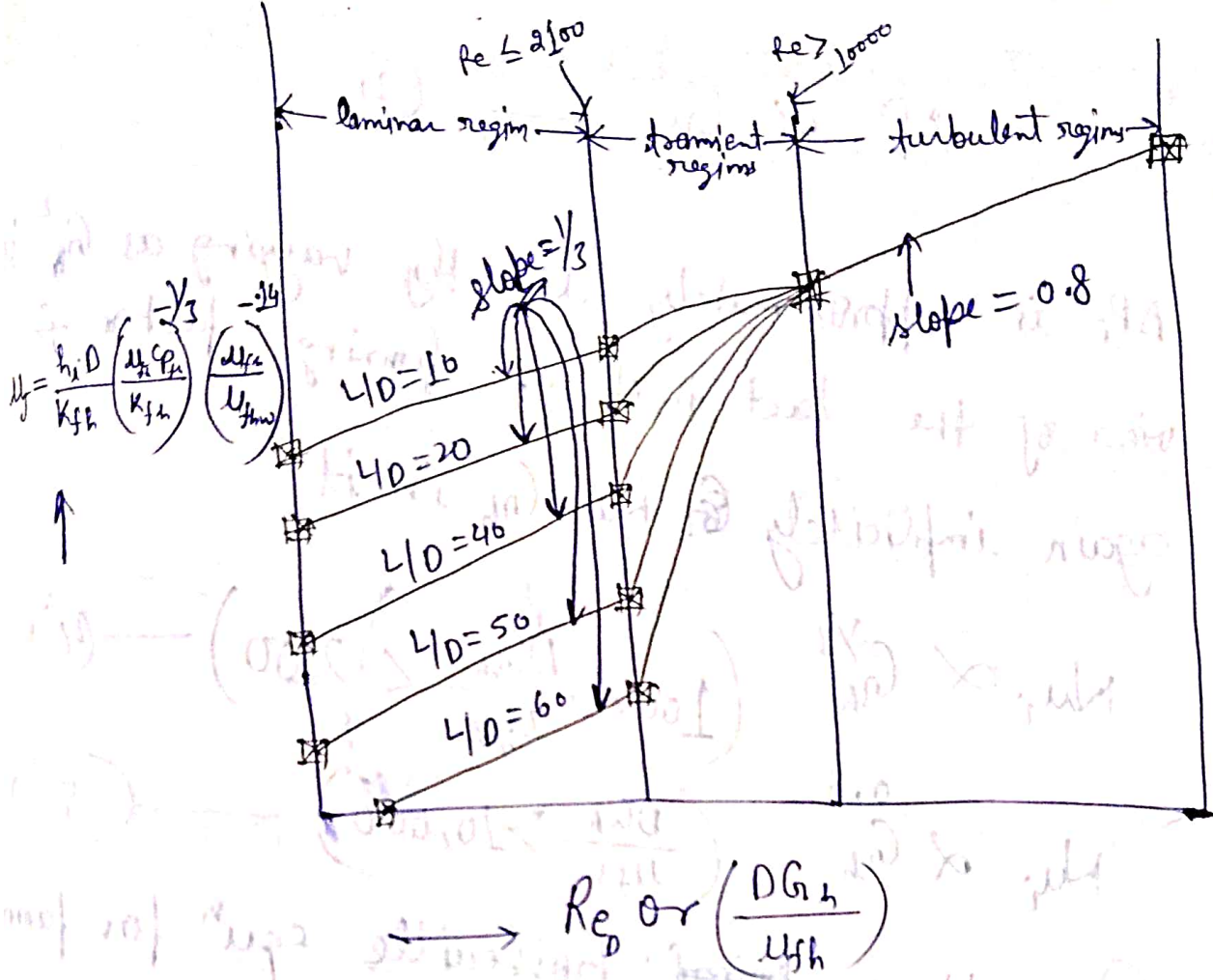
$$h_i \times (\pi DL) = h_{i0} (\pi D_{\perp} L)$$

$$h_{i0} = h_i \left(\frac{D}{D_{\perp}} \right) \quad \text{--- } W/m^2 \cdot K \quad \text{--- (4)}$$

* Pictorial representation of Sieder and Tate

relation for laminar and turbulent

regime \rightarrow



2] Pressure drop calculation for inner pipe fluid:

The press drop, ΔP_i ,

$$\text{across the inner pipe} = C_f \times L/D \times \frac{1}{2} \rho U^2 \quad \text{--- (1)}$$

\uparrow
 friction factor = $4 \times f$
fanning factor

$$= 4f \times \frac{L}{D} \times \frac{1}{2} \rho U^2 \times \frac{\rho}{\rho}$$

$$= \frac{2f L G_h^2}{\rho_h \times D} \quad \text{--- (2)}$$

The above is also called fanning eqⁿ for press^r drop.

$$\Delta P \propto G_{th}^2 \quad \text{--- (3)}$$

ΔP_i is approximately directly varying as G_{th}^2 is view of the fact that the friction factor f again implicitly has G_{th} in it.

$$Nu_i \propto G_{th}^{1/3} \quad \left(100 \leq \frac{DG_{th}}{\mu_{fh}} < 2100 \right) \quad \text{--- (4)}$$

$$Nu_i \propto G_{th}^{0.8} \quad \left(\frac{DG_{th}}{\mu_{fh}} > 10,000 \right) \quad \text{--- (5)}$$

(a) The Hagen ~~poiseuille~~ Poiseuille equation for friction factor : —

$$\frac{DG_{th}}{\mu} < 2100 \Rightarrow \text{Laminar or (streamline flow)}$$

$$f = \frac{16}{Re_D} = \frac{16}{\left(\frac{DG_{th}}{\mu_{fh}} \right)} \quad \text{--- (6)}$$

(b) For $Re_D \left(\frac{DG_{th}}{\mu_{fh}} \right) > 10000$; for all kinds of tubes or pipe : — (The relation given by Drew, Koo and Mc Adams)

$$f = 0.0014 + \frac{0.125}{\left(\frac{DG_{th}}{\mu_{fh}} \right)^{0.32}} \quad \text{--- (7)}$$

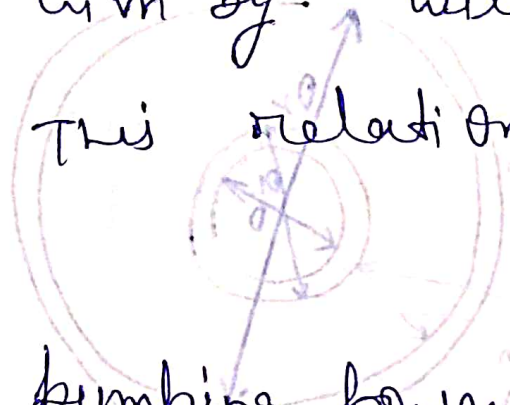
The above relation has a S.D. $\pm 5\%$.

© Specifically for commercial steel and Iron pipes used in industrial application: for $\left(\frac{D G_h}{\mu_{fh}}\right) > 10000$

$$f = 0.0035 + \frac{0.264}{\left(\frac{D G_h}{\mu_{fh}}\right)^{0.42}} \quad \text{--- (8)}$$

Given by: Wilson, Seltzer and Mc Adams.

This relation has a S.D. of $\pm 10\%$.



The pumping power needed to be expanded.

for inner pipe fluid

$$P_i = \Delta P_i \times Q_i \quad \text{--- Watts}$$

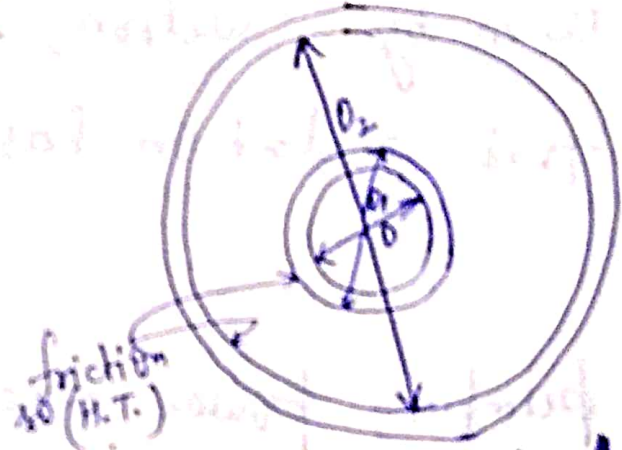
$$Q_i = \pi/4 \cdot D^2 \times U$$

$\frac{(\frac{D^2}{4} \times \pi) \times A}{(\frac{D^2}{4} \times \pi)} = \dots$ } The equivalent diameter for heat transfer calculation = D

$\frac{(\frac{D^2}{4} \times \pi) \times A}{(\frac{D^2}{4} \times \pi)} = \dots$ } The equivalent diameter for fluid flow calculation = D

Blm coeffⁿ and pressure drop in annulus type flow

The equivalent dia or (hydraulic dia) is to be calculated to make use of pipe relation as given already.



It can be noticed from the figure that H.T. b/w the inner pipe and annulus fluid occurs at the outer surface of inner pipe and inner surface of outer pipe becz it encounter friction both at outer surface of inner pipe and inner surface of outer pipe.

$$D_e = \left. \begin{array}{l} \text{The equivalent diameter} \\ \text{for heat transfer calculation} \end{array} \right\} = \sqrt{4 \times \frac{\pi/4 (D_2^2 - D_1^2)}{\pi D_1}} \quad \text{--- (9)}$$

$$\Rightarrow \left(\frac{D_2^2 - D_1^2}{D_1} \right) \text{--- (m)}$$

$$D' = \left. \begin{array}{l} \text{The equivalent diameter} \\ \text{for fluid flow calculation} \end{array} \right\} = \frac{4 \times \pi/4 (D_2^2 - D_1^2)}{\pi (D_1 + D_2)}$$

$$= \frac{(D_2 - D_1) \text{--- (m)}}{1.5}$$

now The Reynold's number for annulus fluid is to be calculated as $\left(\frac{D_e G_c}{\mu_{fc}}\right)$ for H.T. Calculation and $\left(\frac{D_e' G_c}{\mu_{fc}}\right)$ for fluid flow calculation. Then based on value obtained in each case the appropriate relation is to be selected for

Nu_a or h_o and ΔP_a and P_a .

The overall H.T. coefficient based on the outer surface of inner pipe on neglecting the wall resistance.

$$\frac{1}{U_o} = \frac{1}{h_{io}} + \frac{1}{h_o}$$

$$\frac{1}{U_o} = \frac{h_o + h_{io}}{h_o h_{io}} \quad m^2 K/w \quad \text{--- (1)}$$

upon usage over a period of time, the surface of heat exchanger get fouled and empirically given fouling factors have to be taken into account. defining R_{di} and R_{do} are the

~~dist~~ dist factor or fouling factor (fouling resistance) pertaining to inner pipe fluid and outer pipe fluid respectively in $m^2 K/watt$.

The overall H.T. coefficient given by, fouled or inhibited overall H.T. coefficient (U_o')

$$\frac{1}{U_o'} = \frac{1}{U_o} + R_{di} + R_{do} = \frac{1}{h_{i0}} + \frac{1}{h_o} + R_{di} + R_{do} = \frac{1}{U_o} + R_d \quad (12)$$

where $R_d \rightarrow$ net dirt or fouling factor pertaining to both pipe and annulus fluid.

$$R_d = \frac{1}{U_o'} - \frac{1}{U_o}$$

$$R_d = \frac{U_o - U_o'}{U_o U_o'} \quad \text{m}^2 \text{K/w} \quad (13)$$

The rate of heat exchange pertaining to Hair pin HX at the outer surface of the inner pipe is given by

$$q = U_o' \times (\pi D_o L) \times \text{LMTD}_{\text{true}} \quad (14)$$

$$\text{where } \text{LMTD}_{\text{true}} = f \times (\text{LMTD}) \quad (15)$$

$\text{LMTD}_{\text{true}} \rightarrow$ obtain for the same terminal temp^r as per Hair pin HX, and

$f \rightarrow$ being the correction factor generally given empirically in HX practice.

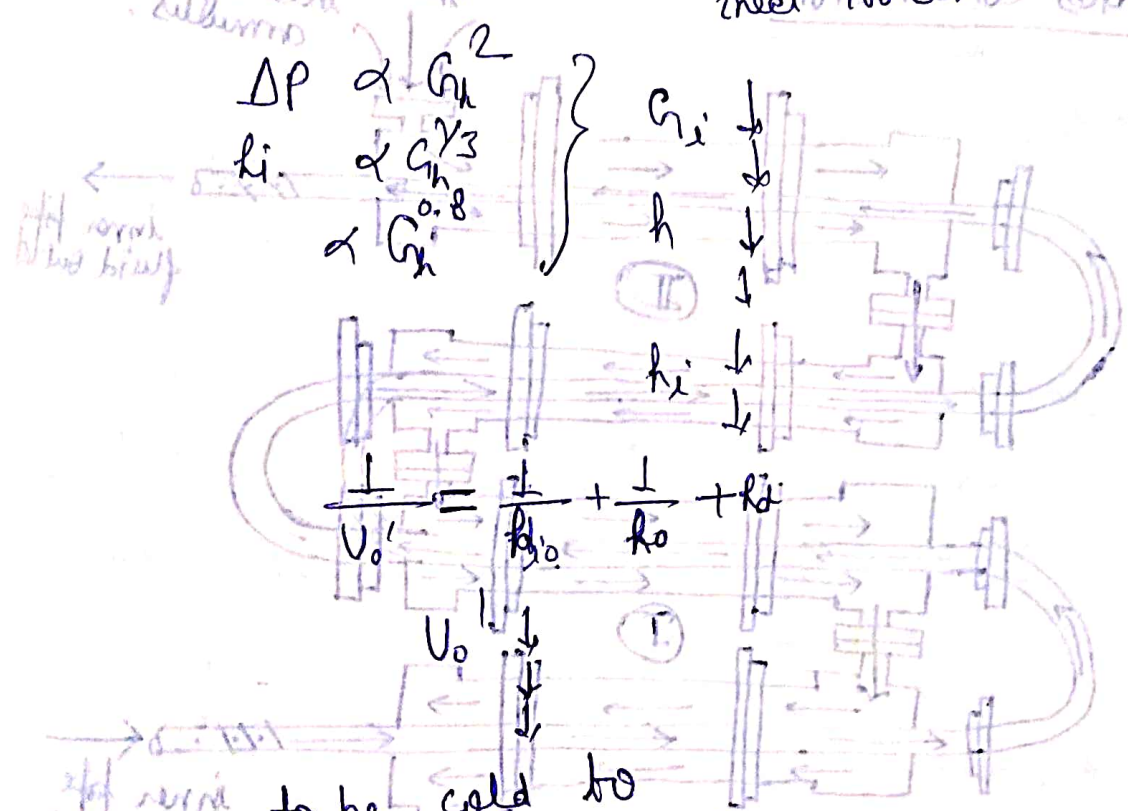
Modifications to hair-pin heat exchanger →

if ΔP_i OR $\Delta P_a \gg \begin{matrix} (\Delta P_i)_{\text{available}} \\ \text{OR} \\ (\Delta P)_{\text{available}} \end{matrix}$ then we will

take inner pipe fluid as a hot fluid.

1/3rd fluid in bypass. → process application

2/3rd fluid through inner pipe. inlet 100°C & anticipated 40°C.

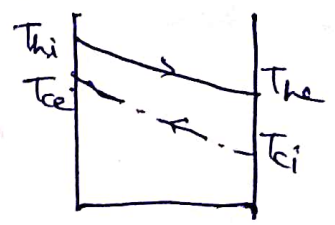


$\Delta P \propto G_h^2$
 $h_i \propto G_h^{0.8}$

$\frac{1}{U_o} = \frac{1}{h_o} + \frac{1}{h_o} + R_i$

to be cold to $T_{in} < 40^\circ\text{C}$

so LMTD ↓



$q = U_o \cdot \underbrace{(\pi D L)}_A \cdot \text{LMTD}$

so Area will be increased & it will be cause of bulkyness of HX.

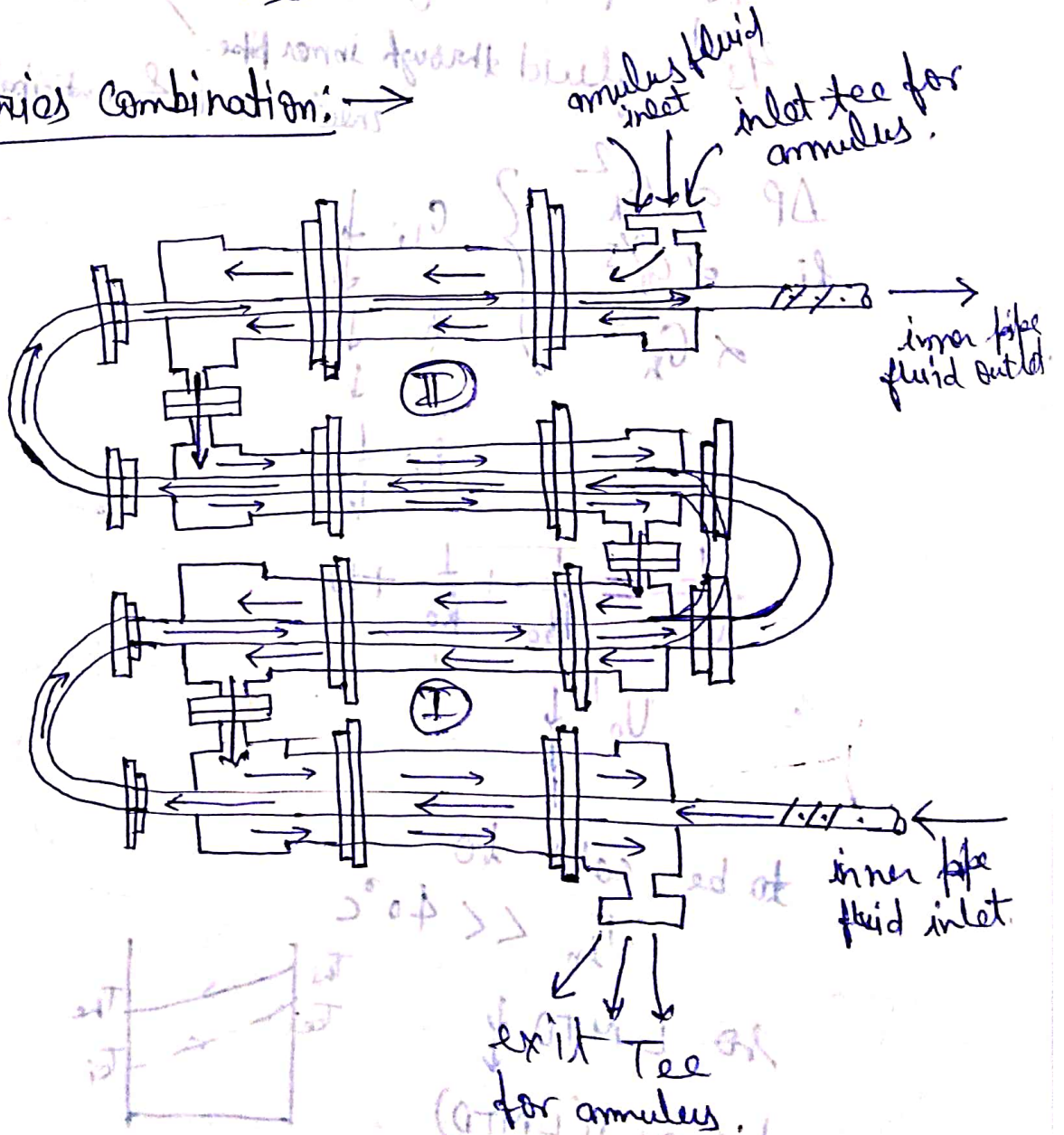
Modification of HX of Hair-pin \rightarrow

Bypass $\Rightarrow X$

① series combination of HX

② Parallel combination of Hair pins

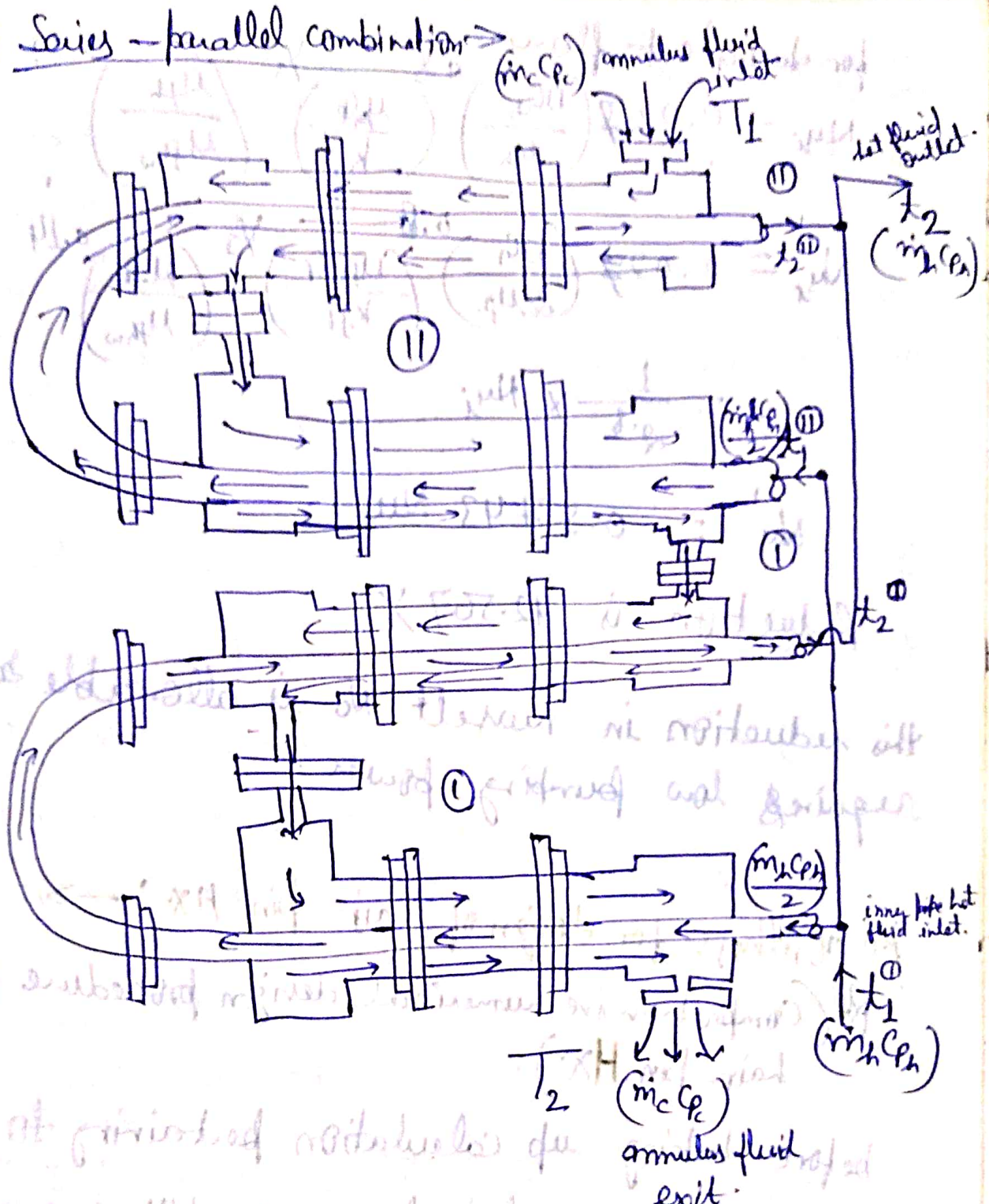
① Series Combination: \rightarrow



Limit of series combination of HX is determined by

$$U_1 A_1 = U_2 A_2 = U_3 A_3 = U_4 A_4 = U_5 A_5 = U_6 A_6 = U_7 A_7 = U_8 A_8 = U_9 A_9 = U_{10} A_{10}$$

9) Series-parallel combination →



Summing equation of pressure drop →

$$\Delta P_i = \frac{2fL \times G_h^2}{\rho_{fh} \times D} \quad \text{--- (1)}$$

for series → $L = L/2$ & $G_h = G_h/2$

$$\Delta P_i' = \frac{2f \frac{L}{2} \times \left(\frac{G_h}{2}\right)^2}{\rho_{fh} \times D} = \frac{1}{8} \times \frac{2fL G_h^2}{\rho_{fh} \times D}$$

$$= \frac{1}{8} (\Delta P_i)$$

for turbulent flow

$$Nu_i = 0.027 \left(\frac{D_{ch}}{\mu_{fh}} \right)^{0.8} \left(\frac{\mu_{fp}}{k_{fh}} \right)^{1/3} \left(\frac{\mu_{fh}}{\mu_{fhw}} \right)^{0.14}$$

$$Nu'_i = 0.027 \left(\frac{D_{ch}}{2\mu_{fh}} \right)^{0.8} \left(\frac{\mu_{fh} C_p}{k_{fh}} \right)^{1/3} \left(\frac{\mu_{fh}}{\mu_{fhw}} \right)^{0.14}$$

$$= \frac{1}{2^{0.8}} \times Nu_i$$

$$Nu'_i = 0.5743 Nu_i$$

Reduction is 42.567%

this reduction in nusselt No is allowable bec it requires low pumping power.

Algorithms for design of Hair-pin HX: →

off (Comprehensive numerical design procedure for hair-pin HX)

before taking up calculation pertaining to Hair-pin HX, certain process conditions are to be identify. firstly — it is to be known ~~weather~~ as to which fluid either the hot or cold flows through inner pipe and annulus, secondly — (it is to be known as to what kind of fluids are used and probable to dirt or fouling factor.

$$Nu_j = 0.027 \left(\frac{D_G}{2\mu_{f,i}} \right)^{0.8} \left(\frac{\mu_{f,i} C_p}{k_{f,i}} \right)^{1/3} \left(\frac{\mu_{f,i}}{\mu_{f,w}} \right)^{0.14}$$

$$= \frac{1}{2^{0.8}} \times Nu_i$$

$$Nu = 0.5743 Nu_i$$

Reduction is 42.567%.

This reduction in result h_0 is allowable because it requires less pumping power.

Algorithms for design of Hair-pin HX: →

OR (Comprehensive numerical design procedure for Hair-pin HX)

before taking up calculation pertaining to Hair-pin HX, certain process conditions are to be identified. firstly — it is to be known ~~whether~~ as to which fluid either the hot or cold flows through inner pipe and annulus, secondly — (it is to be known as to what kind of fluids are used and probable ~~to~~ dirt or fouling factor.

The next information will be regarding standard for both inner pipe and annulus, that helps in arriving @ the design length @ later stage.

let T_1 and T_2

the inlet and exit temp^r of hot fluid ~~by~~
while t_1 and t_2 pertaining to cold fluid.

ρ , C_p , μ , ν , k and Pr indicate mass density, sp. heat @ const press^r, absolute viscosity, kinematic viscosity, thermal conductivity and Prandtl number for each of the fluids. let suffix 'h' and 'c' for hot and cold fluid respectively.

Step 1

(I) Calculation of design length \rightarrow Calculate the

~~(1)~~ ⁽¹⁾ mean temp^r of hot and cold fluid.

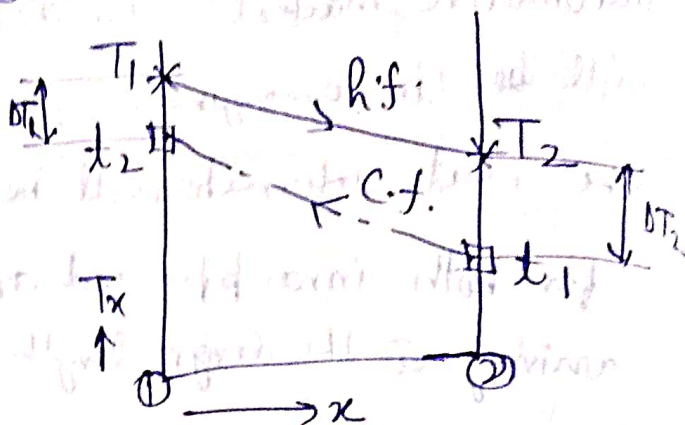
$$\text{By } T_m = \frac{1}{2} (T_1 + T_2)$$

$$t_m = \frac{1}{2} (t_1 + t_2)$$

and extract all the thermophysical properties @ the above temp^r for the fluids concerned.

② assuming the HX to be single pass counter current HX, calculate LMTD as

$$LMTD_{HX} = \frac{\Delta T_1 - \Delta T_2}{\ln \left(\frac{\Delta T_1}{\Delta T_2} \right)}$$



③ from empirically provided value for correction factor which is typically in the range of 0.85 to 0.95. Calculate $LMTD_{true}$

$$LMTD_{true} = F_X LMTD_{HX}$$

④ inner pipe calculation: →

$$q_p = \frac{\pi}{4} D^2$$

subsequently the mass flow rate inner pipe fluid know as m_h or (m_c) the

$$\text{mass velocity } G_p = \frac{m_h \text{ or } (m_c)}{q_p} \text{ kg/m}^2$$

⑤ Calculate Reynolds number for inner pipe fluid as $\frac{D G_p}{\mu}$ & check for its Range.

if $100 \leq \frac{D G_p}{\mu} \leq 2100$

for laminar.

if $\frac{D G_p}{\mu} > 10000$

for turbulent

⑥ using appropriate film

Coefficient for inner pipe fluid (based on inner surface of inner pipe).

~~For laminar~~

$$Nu_i = \frac{h_i D}{k_{fh}} = 1.86 \left(\frac{D G_p}{\mu_{fh}} \right) \left(\frac{\mu_{fh} C_{p, fh}}{k_{fh}} \right) \left(\frac{D}{L} \right)^{1/3} \times \left(\frac{\mu_{fh}}{\mu_{fw}} \right)^{0.14}$$

OR for turbulent \rightarrow

$$Nu_i = \frac{h_i D}{k_{fh}} = 0.027 \left(\frac{D G_p}{\mu_{fh}} \right)^{0.8} \left(\frac{\mu_{fh} C_{p, fh}}{k_{fh}} \right)^{1/3} \left(\frac{\mu_{fh}}{\mu_{fw}} \right)^{0.14}$$

⑦ Using h_i thus obtained calculate film coefficient for inner pipe fluid based on outer surface of inner pipe.

$$h_{io} = h_i \left(\frac{D_i}{D_o} \right) \quad \text{--- } W/m^2 K$$

⑧ Annulus calculation \rightarrow

① flow area of the annulus is calculation

$$q_a = \frac{\pi}{4} (D_2^2 - D_1^2) \quad \text{--- } m^2$$

② mass velocity of annulus fluid is calculated as.

$$G_a = \frac{m_p \text{ or } m_c}{q_a} \quad \text{--- } kg/m^2 s.$$

③ Calculate the equivalent diameter pertaining to heat transfer.

$$D_e = \frac{D_2^2 - D_1^2}{D_1} \quad \text{--- } m.$$

Thus calculate -

$Re = \left(\frac{D_c G_c}{\mu} \right)$ and check for range called the

flow is either laminar or turbulent.

$$100 \leq \frac{D_c G_c}{\mu} \leq 2100 \quad \text{for laminar}$$

$$\frac{D_c G_c}{\mu} > 10,000 \quad \text{for turbulent}$$

(10) Calculate film coefficient base on using appropriate relation as decided as flow is identified (laminar/turbulent)

$$Nu_o = \frac{h_o D}{k} = 1.86 \left[\left(\frac{D G_c}{\mu} \right) \left(\frac{\mu_c}{k} \right) \left(\frac{D}{L} \right) \right]^{1/3} \left(\frac{\mu}{\mu_w} \right)^{0.14}$$

$$Nu_o = \frac{h_o D}{k} = 0.027 \left[\left(\frac{D G_c}{\mu} \right)^{0.8} \times \left(\frac{\mu_c}{k} \right)^{1/3} \left(\frac{\mu}{\mu_w} \right)^{0.14} \right]$$

(11) Calculate using dirt factor R_{di} and R_{do} given empirically, the overall H.T. coefficient using.

$$\frac{1}{U_o'} = \frac{1}{h_{io}} + \frac{1}{h_o} + R_{di} + R_{do} \quad m^2 K/watt$$

after obtaining U_o' and calculated $LMTD_{\text{true}}$

in step (3) finish design calculation by setting: —

$$U_o' \times A_o \times \left(\underset{\Rightarrow \text{true}}{LMTD} \right) = m_h C_{ph} (T_1 - T_2)$$

$$\text{or} = m_c C_{pc} (T_2 - T_1)$$

(12) The above gives A_o , called as H.T. Area based on outer surface of inner pipe which is equal to

$$A_o = \pi D_o \times L_{\text{design}}$$

Calculate L_{design} which is equal to $2L_e$ obtained L_e from above and check within permissible limiting length (12', 15', 20'), & upper limit (40'). If L_e exceeds the upper limit appropriate decides the no. of hair pins are connected in series.

(II) Pressure drop calculation: →

(13) calculate, depending on range in which $\left(\frac{D_{eq}}{\mu} \right)$ is falling, the friction factor using appropriate relation.

~~$$\Delta P_f = C_f \times L \times \frac{1}{2} \rho_{fh} U^2 \times \frac{S_{fh}}{S_{fh}}$$~~

$$\Delta P_f = C_f \times L \times \frac{1}{2} \rho_{fh} U^2$$

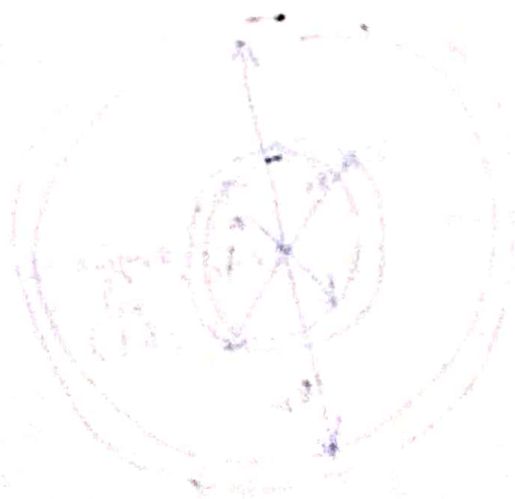
$$C_f = 4f$$

finally eqn for pres^r drop. $\Delta P_f = \frac{2fL C_p^2}{S_{fh} \times D}$

⑬ Calculate ΔP_a used in step ⑭ by forming eqⁿ.

$$\Delta P_a = 2f \frac{L}{D_e} \frac{G_a^2}{\rho f h}$$

⑰ check whether ΔP_i & ΔP_a within flow packing to available pumps for inner pipe and annulus.



⑱

(10)

Ques 5 - a hair-pin HX is proposed to be design for industrial application, inner pipe of HX has cold water flowing through it @ 12 kg/s. Entering and leaving it respectively 25°C and 40°C . where annulus to hot engine oil that enters and leaves the annulus respectively @ temp 70°C and 48°C , estimation within that fouling factor pertaining to inner and outer surfaces of the inner pipe are respectively about $0.0021 \frac{\text{m}^2\text{K}}{\text{W}}$ and $0.0035 \frac{\text{m}^2\text{K}}{\text{W}}$. The inner and outer dia of inner pipe and inner dia of annulus are respectively measured to be 3.5 cm, 4 cm and 5 cm. The correction factor for two temp diff^r is 0.95. Calculate the design length of inner pipe required for the HX. further calculate the pressure drops across the inner pipe and annulus. provide your comments on the various results as above.

Solution →

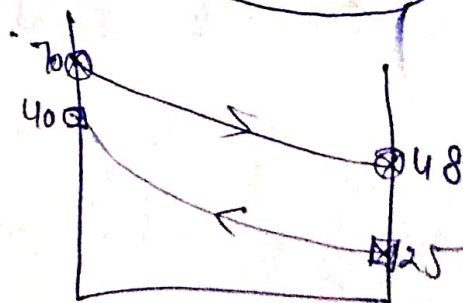
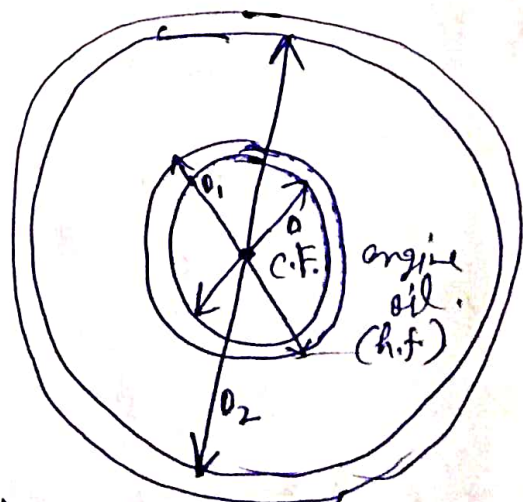
$$D = 0.035 \text{ m}$$

$$D_1 = 0.04 \text{ m}$$

$$D_2 = 0.05 \text{ m}$$

$$\text{LMTD} = \frac{30 - 23}{\ln(30/23)}$$

$$\text{LMTD} = 26.35^{\circ}\text{C}$$



$$x_1 = 25^\circ\text{C}, x_2 = 40^\circ\text{C}, T_1 = 70^\circ\text{C}, T_2 = 48^\circ\text{C}$$

$$f = 0.95; R_{di} = 0.0021 \text{ m}^2\text{K/W and } R_{do} = 0.0035 \text{ m}^2\text{K/W}$$

$$\dot{m}_c = 12 \text{ Kg/s and } \dot{m}_h = ?$$

Calculation →

a) $t_{\text{mean}} = \frac{1}{2}(x_1 + x_2) = 32.5^\circ\text{C}$

b) $T_{\text{mean}} = \frac{1}{2}(T_1 + T_2) = 59^\circ\text{C}$

now we will calculate the properties for t_{mean} and T_{mean} by using interpolation

Temp	ρ (kg/m ³)	ν (m ² /s)	Pr	K (W/mK)	Cp
20°C	1000	1.006×10^{-6}	7.020	0.5978	4178
40	995	0.657×10^{-6}	4.34	0.6280	4178
32.5	996.875	0.7878×10^{-6}	5.345	0.6167	4178

$\mu_c = 7.854 \times 10^{-4} \text{ N s/m}^2$ for water →

$\mu_{wc} @ 59^\circ\text{C} \quad \nu = \frac{\mu}{\rho}$

$\mu_{wc} = 479.88 \times 10^{-6}$

$\mu_{wc} = 4.7988 \times 10^{-4} \text{ N s/m}^2$

Temp	ν	ρ
40	0.657×10^{-6}	995
60	0.478×10^{-6}	985
59	0.48695×10^{-6}	985.5

$\mu_h = 7.859 \times 10^{-2} \text{ N s/m}^2$

Prandtl No →

Temp	ν (m ² /s)	ρ (kg/m ³)	Pr	K (W/mK)	Cp
40	241×10^{-6}	876	2870	0.1442	1964
60	83×10^{-6}	864	1250	0.1407	2047
59	90.9×10^{-6}	864.6	1141	0.140875	2042.85

$$\mu_{w,h} @ 32.5^\circ\text{C}$$

$$\mu_{w,h} = 0.4301 \text{ N}\cdot\text{s}/\text{m}^2$$

$$\dot{m}_h c_{p,h} (T_1 - T_2) = \dot{m}_c c_{p,c} (t_2 - t_1)$$

$$\dot{m}_h \times 2042 (70 - 48) = 16 \times 4178 (40 - 25)$$

$$\dot{m}_h = 16.7333 \text{ kg/s}$$

$$q = \dot{m}_h c_{p,h} (T_1 - T_2)$$

$$q = 16.73333 \times 2042 (70 - 48)$$

$$q = 752040 \text{ W}$$

@ as we

$$\text{LMTD} = 26.35^\circ\text{C}$$

$$\text{LMTD}_{\text{true}} = 26.35 \times 0.95$$

$$\text{LMTD}_{\text{true}} = 25.03^\circ\text{C}$$

Calculate inner pipe related film coefficient h_i & h_o :-

$$G_p = \frac{\dot{m}c}{a_p} = \frac{12}{\frac{\pi}{4} \times (0.035)^2}$$

$$G_p = 12472.55 \text{ kg/m}^2\text{s}$$

$$Re = \frac{D G_p}{\mu_c} = \frac{0.035 \times 12472.55}{7.854 \times 10^{-4}}$$

$$\boxed{Re = 555817.7648} \text{ flow will be turbulent}$$

$$Nu_x = \frac{h_x D}{k_f} = 0.027 \left(\frac{D G_p}{\mu_x} \right)^{0.8} \left(\frac{\mu_x \times C_{p_h}}{k_{f_h}} \right)^{1/3} \left(\frac{\mu_h}{\mu_x} \right)^{0.14}$$

$$\frac{h_x \times 0.035}{0.140875} = 0.027 \left(555817.7648 \right)^{0.8} \left(\frac{7.854 \times 20428}{0.140875} \right)^{1/3} \left(\frac{7.859 \times 10^{-2}}{7.854 \times 10^{-4}} \right)^{0.14}$$

~~$$h_x = 0.027 \times (555817.7648)^{0.8} \times (113961.776)^{1/3} \times (1.90563)$$~~

$$h_x = (4286.23) \times (10.4412) \times (1.9056)$$

$$h_x = 35149.38 \text{ W/m}^2\text{K}$$

$$h_{i0} \times D_L = h_i \times D$$

$$\boxed{h_{i0} = 30753.8319 \text{ W/m}^2\text{K}}$$

$$q_a = \frac{\pi}{4} (0.05^2 - 0.04^2)$$

$$q_a = 7.0685 \times 10^{-4} \text{ m}^2$$

$$G_a = \frac{m_h}{q_a} = \frac{16.7333}{7.0685 \times 10^{-4}}$$

$$G_a = 23672.819 \text{ kg/m}^2 \cdot \Delta$$

$$D_e = \frac{D_2^2 - D_1^2}{D_1} \text{ (m)}$$

$$D_e = 0.0225 \text{ m}$$

$$\frac{D_e G_a}{\mu_h} = \frac{0.0225 \times 23672.819}{7.859 \times 10^{-2}}$$

$$\frac{D_e G_a}{\mu_h} = 6777.43$$

Since the above value is closer to 10000 than to 2500 it is fairly accurate for turbulent flow

$$Nu_{ho} = \frac{h_o \times D_e}{k_f} = 0.027 \left(\frac{D_e G_a}{\mu} \right)^{0.8} \left(\frac{\mu_{ho}}{k} \right)^{1/3} \left(\frac{\mu_h}{\mu_w} \right)^{1/4}$$

$$\frac{h_o \times 0.0225}{0.140875} = 0.027 \left(6777.43 \right)^{0.8} \left(\frac{7.859 \times 10^{-2} \times 23672.819}{0.140875} \right)^{1/3} \times \left(\frac{7.859 \times 10^{-2}}{7.854 \times 10^{-2}} \right)^{1/4}$$

$$h_0 = (196.276) \times (1139.6177) \times (1.9056)$$

$$h_0 = 1616.462 \text{ W/m}^2\text{K}$$

$$\frac{1}{U_1} = \frac{1}{h_{i0}} + \frac{1}{h_0} + R_{di} + R_{do}$$

$$\frac{1}{U_0} = \frac{1}{30753.8319} + \frac{1}{1616.462} + 0.0002 + 0.0035$$

$$U_0 = 159.97 \text{ W/m}^2\text{K}$$

$$q = 752040 \text{ W} = U_0 \times A \times (LMTD)$$

$$A_0 = 187.83 \text{ m}^2$$

$$A_0 = \pi D_1 L$$

$$L = \frac{187.83}{\pi \times 0.035}$$

$$L = 1494.70 \text{ m}$$

$$= 2L_e$$

$$L_e = 747.35 \text{ m}$$

Considering the upper limit of effective length

$$(L_e)_{\text{upper limit}} = \frac{20 \times 12 \times 2.54}{100} = 6.096 \text{ m}$$

The value of NP_1 and NP_2 is based on the value of L obtained in the initial calculation. If they appear to be fairly large, it is likely to bring down when combination of hair pins is used.

CHAPTER-6

Shell and Tube HX! →

When ever we required larger H.T. rate and the two drawbacks of Hair-pin HX are -

- ① The Hair-pin HX connects in series so the area is larger & it becomes bulky.
- ② The leakage problem occurs.

a shell and tube heat exchanger tries to address the twin problems of -

- ① Requirement of larger floor area owing to bulkiness.
- ② Large no. of vulnerable leakage points that arises when one is made to use a no. of HX to meet larger HX loads.



Design of plate heat exchangers

Prashant Saini

Mechanical Engineering Department

***Madan Mohan Malaviya University of
Technology Gorakhpur (UP State Govt. University)***

Email: psme@mmmut.ac.in



Rankine Cycle

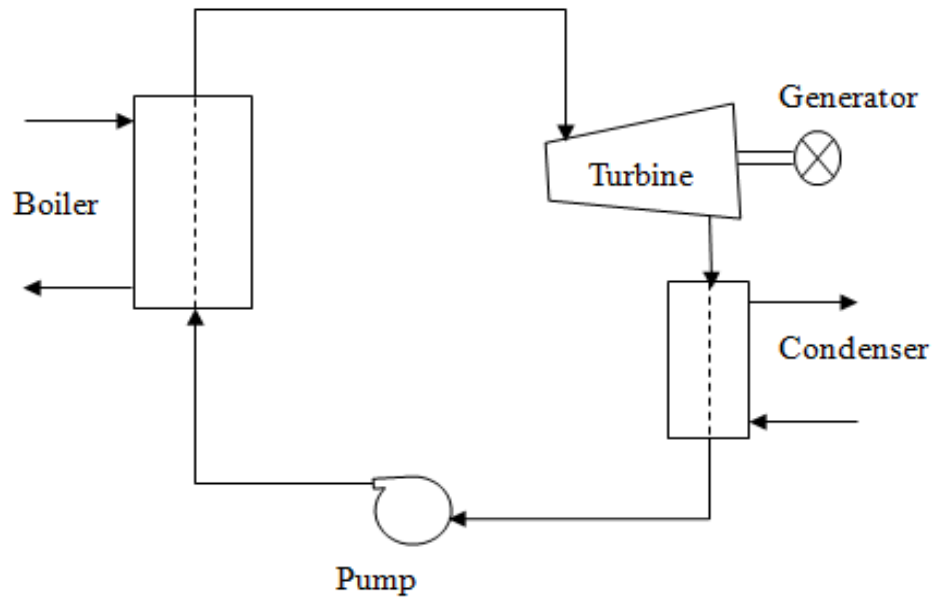


Fig. 1. Schematic diagram of an ORC.

Main Components of Rankine cycle:

1. Vapor generator
2. Turbine
3. Condenser
4. Pump



T-s diagram of working fluids

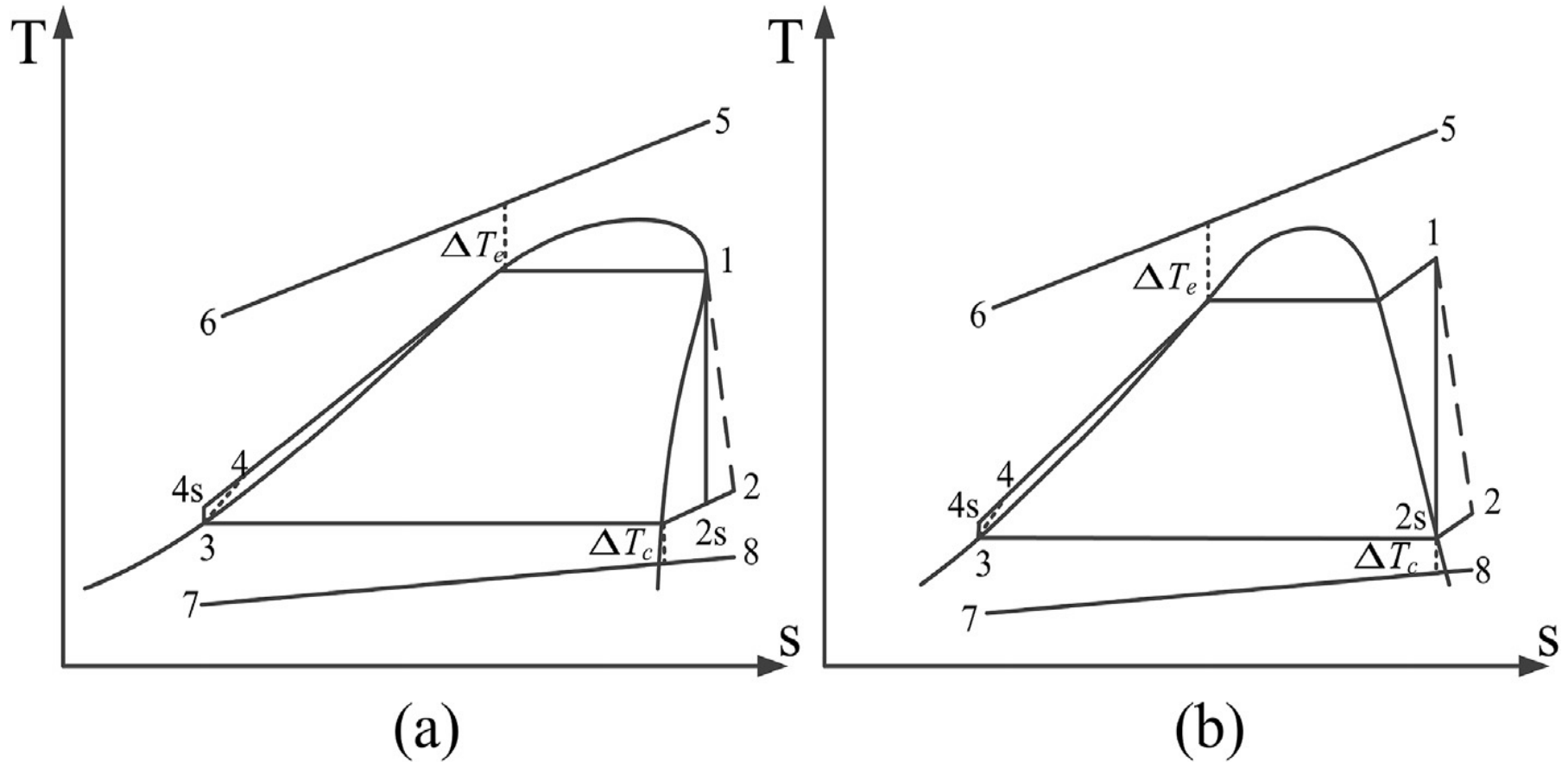


Fig. 2. T-s diagram of working fluids: (a) dry or isentropic and (b) wet.



Various zone of vapor generator and condenser

Vapor generator is divided into three regions, i.e. preheating, evaporation and superheating region while condenser is divided into two regions, i.e. cooling and condensation region as shown in Fig. 3

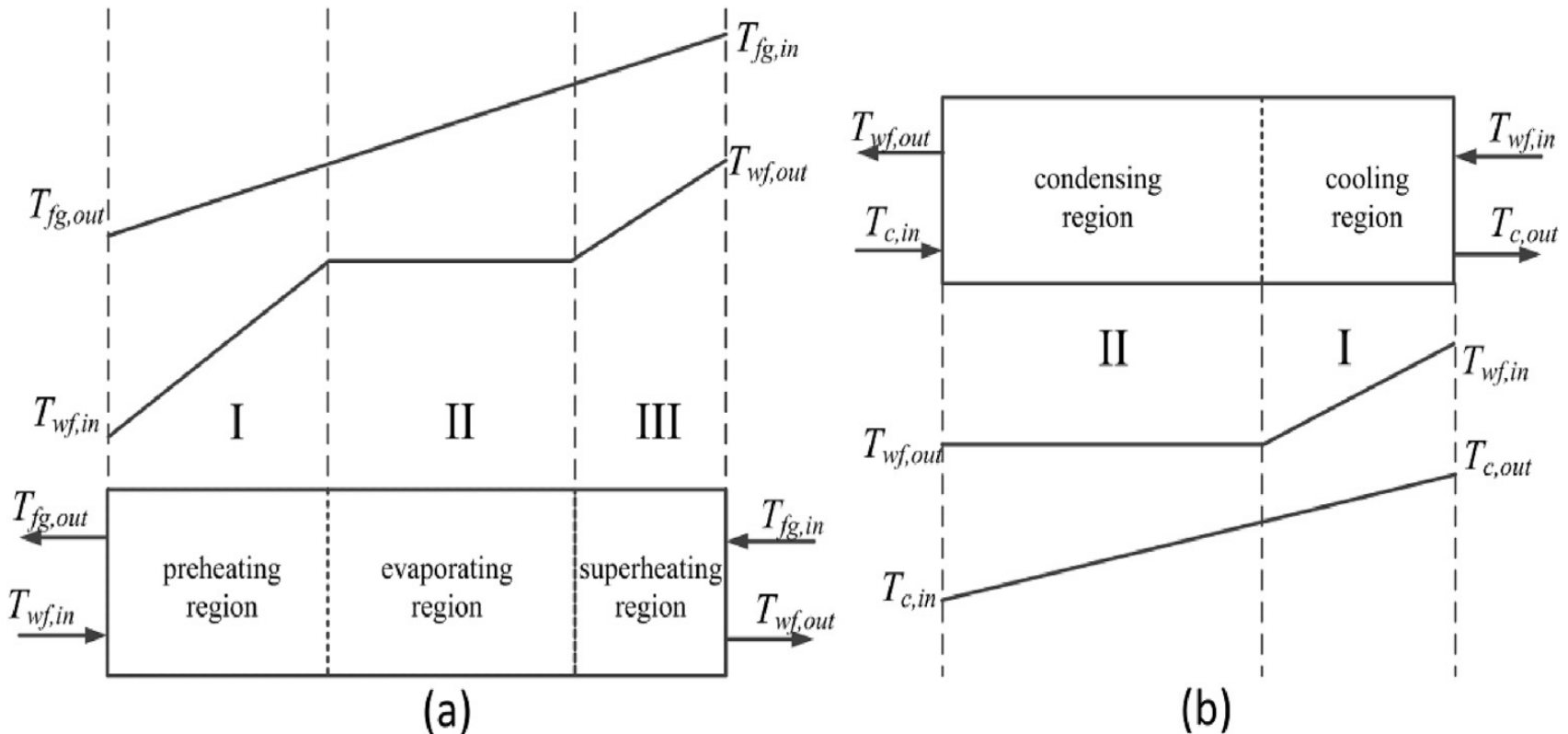


Fig. 3. Three-zone modeling of an vapor generator (a) and two-zone modeling of a condenser (b).



Calculation of Overall H. T. Coefficient and H.T. area

Single-phase region: $Q_{sp} = U_{sp} A_{sp} LMTD_{sp}$

The overall heat transfer coefficient of single phase for plate heat exchangers:

Component	Overall heat transfer coefficient	Heat exchange area	Total area
Vapor generator:			
Single-phase region	$\frac{1}{U_{vg,1}} = \frac{1}{\alpha_{sp,o}} + \frac{t}{k_{plate}} + \frac{1}{\alpha_{sp,wf}}$	$A_{vg,1} = \frac{Q_{vg,1}}{U_{vg,1} \times LMTD_{vg,1}}$	$A_{vg} = A_{vg,1} + A_{vg,2}$
Two-phase region	$\frac{1}{U_{vg,2}} = \frac{1}{\alpha_{sp,o}} + \frac{t}{k_{plate}} + \frac{1}{\alpha_{tp,wf}}$	$A_{vg,2} = \frac{Q_{vg,2}}{U_{vg,2} \times LMTD_{vg,2}}$	
Condenser:			
Single-phase region	$\frac{1}{U_{cr,1}} = \frac{1}{\alpha_{sp,w}} + \frac{t}{k_{plate}} + \frac{1}{\alpha_{sp,wf}}$	$A_{cr,1} = \frac{Q_{cr,1}}{U_{cr,1} \times LMTD_{cr,1}}$	$A_{cr} = A_{cr,1} + A_{cr,2}$
Two-phase region	$\frac{1}{U_{cr,2}} = \frac{1}{\alpha_{sp,w}} + \frac{t}{k_{plate}} + \frac{1}{\alpha_{tp,wf}}$	$A_{cr,2} = \frac{Q_{cr,2}}{U_{cr,2} \times LMTD_{cr,2}}$	



Calculation of convection H. T. Coefficient

For all single-phase flow, Muley correlation [38] is used to determine the convection heat transfer coefficients. This correlation is valid for a specific range of equivalent Reynolds number ($30 \leq Re \leq 400$) and chevron angle ($\pi/6 \leq \beta \leq \pi/3$).

$$Nu = \frac{D_{eq}\alpha_{sp}}{k_{plate}} = 0.44 \left(\frac{6\beta}{\pi}\right)^{0.38} Re_{eq}^{0.5} Pr^{1/3} \left(\frac{\mu}{\mu_{wall}}\right)^{0.14}$$

For all two-phase flow, Yan-Lin correlation [38,39] is used to determine the convection heat transfer coefficients. This correlation is valid for a specific range of equivalent Reynolds number ($2000 \leq Re \leq 10000$).

$$Nu = \frac{D_{eq}\alpha_{tp}}{k_{plate}} = 1.926 Re_{eq}^{0.5} Pr^{1/3} Bo_{eq}^{-0.3} [1 - x + x(\rho_l/\rho_v)^{0.5}]$$



Contd...

Where:

- $Re_{eq} = \frac{G_{eq} D_{eq}}{\mu}$

- $Bo_{eq} = \frac{q''_{wall}}{G_{eq} h_{fg}}$

- $G_{eq} = G [1 - x + x(\rho_l/\rho_v)^{0.5}]$

The pressure drops are expressed as:

- $\Delta p = 2 * f * (G * G) / \rho * Dh$

- $f = 14.62 * Re^{-0.514}$ $Re \leq 50$

- $f = 2.21 * Re^{-0.097}$ $Re \leq 180$

THANK YOU



Assessment of boiling and condensation heat transfer correlations in the modelling of plate heat exchangers

J.R. García-Cascales^{a,*}, F. Vera-García^a, J.M. Corberán-Salvador^b,
J. González-Maciá^b

^a*Thermal and Fluid Engineering Department, Universidad Politécnica de Cartagena, 30202 Cartagena, Murcia, Spain*

^b*Applied Thermodynamics Department, Universidad Politécnica de Valencia, Spain*

Received 4 September 2006; received in revised form 7 November 2006; accepted 9 January 2007

Available online 18 January 2007

Abstract

This paper studies refrigeration cycles in which plate heat exchangers are used as either evaporators or condensers. The performance of the cycle is studied by means of a method introduced in previous papers which consists of assessing the goodness of a calculation method by looking at representative variables such as the evaporation or the condensation temperature depending on the case evaluated. This procedure is also used to compare several heat transfer coefficients in the refrigerant side. As in previous works the models of all the cycle components are considered together with the heat exchanger models in such a way that the system of equations they provide is solved by means of a Newton–Raphson algorithm. Calculated and measured values of the evaporation and the condensation temperatures are also compared. The experimental results correspond to the same air-to-water heat pump studied in other papers and they have been obtained by using refrigerants R-22 and R-290.

© 2007 Elsevier Ltd and IIR. All rights reserved.

Keywords: Refrigeration; Air conditioning; Heat exchanger; Survey; Correlation; Condensation; Heat transfer; Comparison; Experiment

Evaluation des corrélations de transfert de chaleur lors de l'ébullition et de la condensation dans la modélisation des échangeurs de chaleur à plaque

Mots clés : Réfrigération ; Conditionnement d'air ; Échangeur de chaleur ; Enquête ; Corrélation ; Condensation ; Transfert de chaleur ; Comparaison ; Expérimentation

1. Introduction

This work is part of a series that studies the performance of a refrigeration cycle model by estimating cycle parameters such as the evaporation or the condensation

* Corresponding author. Tel.: +34 968 325 991; fax: +34 968 325 999.

E-mail address: jr.garcia@upct.es (J.R. García-Cascales).

Nomenclature

a_1, a_2, a_3, a_4	adjustment correlation parameters	x	vapour quality.
B_1, B_2	empirical constants in Bogaert and Böles correlation	<i>Greeks</i>	
Bo	boiling number	α	heat transfer coefficient ($\text{W}/\text{m}^2 \text{K}$)
c_1, c_2, c_3	correlation parameters	β	chevron angle (radian)
C_1, C_2, C_3, C_4	Yan–Lin correlation coefficients	η	dynamic viscosity ($\text{N s}/\text{m}^2$)
Co	convection number	ϕ	enlargement factor
d_1, d_2	correlation parameters	ρ	density (kg/m^3)
D	diameter (m)	<i>Subscripts and superscripts</i>	
D_h	hydraulic diameter (m)	cb	convective boiling
f	friction factor	cp	previously calculated
f_0, f_1	Martin correlation parameters	eq	equivalent
F	enhancement factor	f	saturated liquid (liquid phase)
Fr	Froude number	g	saturated vapour (vapour phase)
G	mass velocity ($\text{kg}/\text{s m}^2$)	h	hydraulic
Ge_1, Ge_2	Han–Lee–Kim correlation coefficients	l	laminar
i	enthalpy (J/kg)	l	liquid
j	heat transfer coefficients in Wanniarachchi correlation	lo	liquid only
Nu	Nusselt number	m	in the middle of the fluid flow
p	pressure (Pa)	nb	nucleate boiling
p_{co}	heat exchanger pitch	r	refrigerant
Pr	Prandtl number	sat	saturation
q	heat flux (W/m^2)	t	turbulent
Re	Reynolds number	tp	two-phase flow
S	suppressing coefficient	w	wall
		*	reduced

temperature. It focuses on the study of the influence of heat transfer coefficient models in plate heat exchanger modelling. This study is justified by the leading role that these heat exchangers now play in certain applications. They are being used intensively mostly due to the great amount of advantages that they have with respect to their competitors. They are easily cleaned, inspected, and maintained and high turbulence can be achieved without great effort, thus the required surface and the volume occupied are much lower than those needed by a shell and tube exchanger for the same duty (high compactness). This justifies their use in many industrial applications. They have been utilised widely in liquid-to-liquid applications and have been used as evaporators and condensers since the last decade basically because of their high effectiveness and low cost [1].

The evaluation of characteristic variables of the cycle such as the evaporation or the condensation temperatures is used to compare several heat transfer coefficients correlations in the refrigerant side. Unlike fin and tube heat exchangers, the secondary fluid resistance (water in this case) is approximately 40% lower than the refrigerant resistance. This makes the calculation of the evaporation or condensation temperatures more sensitive to the correlations used for the refrigerant heat transfer coefficient.

As in previous papers [2,3], the models of all cycle components are considered together, providing a system of equations that is solved by using a Newton–Raphson algorithm. The SEWTLE procedure is used to evaluate the outlet conditions of the heat exchangers [4]. Some experimental data corresponding to an air-to-water heat pump have been used to compare calculated and measured values of the characteristic temperatures mentioned above. The refrigerants used in the experimental facility are R-22 and R-290. The governing equations and the global model used to analyse the refrigeration cycle will not be described here – the interested reader may find a complete description in [4]. The diagrams of the heat pump used to perform the experiment can be found in [2,3].

This paper has been structured as follows. Firstly, a comparative study is carried out describing the heat transfer coefficient used in plate heat exchangers working in single-phase or in two-phase flow, either as evaporators or condensers. Secondly, the experimental results obtained in the heat pump for the evaporation and condensation temperatures are compared with the results provided by the model which is included in the ART[®] code [5]. The methodology described in [2,3] for tube and fin heat exchangers is also applied here and it depends on the element considered, i.e. an evaporator or a condenser.

2. Heat transfer coefficient

Some common heat transfer coefficients applied to the heat transfer characterisation in plate heat exchangers are studied in this section. It focuses on those employed in refrigeration cycles, mostly on the refrigerant side. The amount of available correlations in the existing literature is fairly extensive and, unfortunately, some of these interesting works cannot be described in this paper. The effort made in the characterisation of adiabatic two-phase flow in plate heat exchangers has actually been remarkable [6–10]. Many phenomena and dependencies encountered in the heat transfer coefficient correlations proposed in those references are extrapolable to evaporation or condensation of refrigerants. Correlations developed for subcooled flow boiling heat transfer, such as the one developed by Hsieh–Chiang–Lin in [11] for R-134a in vertical plate heat exchangers, or recent works on vaporisation and condensation inside herringbone plate heat exchanger with enhanced surfaces as [12], should also be highlighted.

In the following sections, a brief review of the single-phase correlations is initially carried out. Then, some two-phase correlations used for the characterisation of the evaporation and condensation processes are presented. All of them have been compared in order to have a better picture of their differences and their range of application. The ranges of heat and mass fluxes used to calculate and compare the heat transfer coefficient values correspond to those encountered in the experiment.

2.1. Single-phase flow

Heat transfer coefficient and pressure drop in plate heat exchangers have been investigated for several years, and the amount of work that has been carried out is quite extensive. A general theory or correlation covering all geometrical parameters and combinations of plate heat exchangers does not exist. The large amount of possible combinations which results from the variation of the geometric parameters of the plate heat exchangers makes such a theory almost impossible.

Each investigation should be regarded as a special case whose results are only applicable for the specific geometry and combinations tested. Unfortunately, this investigation cannot present all geometry parameters in detail.

There are more than 30 practical correlations starting with Troupe et al. [13] in 1960, and continuing up to one of the latest correlations published by Muley and Manglik [14] and Muley et al. [15] in 1999. An exhaustive compilation of some of the most important correlations is made by Ayub [16]. In accordance with him, the majority of the correlations could be used for plates of different manufacturers but he recommends the Kumar correlation [17] for quick calculations, and those by Heavner et al. [18], Wanniarachchi et al. [19] and Muley and Manglik [14,15,20] for more elaborated calculations. Some of them are also

recommended by Claesson [21,22], where the Bogaert and Bölcs [23], Martin [24], Muley and Manglik [14], Muley et al. [15] and Muley [20] correlations are compared. The Bogaert and Bölcs [23] correlation is used by plate heat exchanger manufacturers and this is an adaptation of constants and exponents to experimental data for plate heat exchangers with specific geometries. The correlations developed by Muley and Manglik [14], Muley et al. [15] and Muley [20] are an attempt to generalise the Nusselt number correlation, including dependencies of chevron angle and enlargement factor. The Martin [24] correlation is another attempt to generalise the Nusselt number correlation by applying an analogy between heat transfer and pressure drop. This is a semiempirical correlation as several parameters are fitted to experimental data. Throughout this paper, some of the correlations mentioned above, and others commonly used in plate heat exchanger design have been studied and compared.

Force convection heat transfer coefficients are frequently correlated as

$$Nu = c_1 Re^{c_2} Pr^{c_3} \left(\frac{\eta_m}{\eta_w} \right),$$

where c_1 , c_2 , and c_3 depend on the plate pattern and geometrical parameters.

In the laminar regime, the flow is generally not fully developed in plate exchanger passages, the Leveque correlation, originally proposed for a circular tube, is proposed by some authors

$$Nu = c_4 \left(\frac{L}{D_{eq} Re Pr} \right)^{-1/3} \left(\frac{\eta_m}{\eta_w} \right)^{-0.14}, \quad (1)$$

where c_4 depends on the thermal boundary conditions and the plate geometry. The dependence on the plate length, L , is reported not to be correct by some authors. As confirmed by their experiments, other researchers have proposed a larger exponent on the Reynolds number [1].

Shah and Wanniarachchi report some values for the coefficients c_i [1] taken from other authors' works. Despite this, some of these correlations are of little practical use for plate heat exchanger design since no specific values of these constants are available in the literature for some plate geometry. It is recommended that the influence of the Prandtl number on the Nusselt number be characterised by an exponent of 1/3 for conservatism. It can tend to 0.4 in the case that simultaneously laminar and turbulent flows take place, as may happen in plate heat exchangers. As customary, the influence of temperature-dependent viscosity is expressed by means of a term of

$$\frac{Nu}{Nu_{cp}} = \left(\frac{\eta_m}{\eta_w} \right)^n,$$

Values for n and m may be encountered in Shah and Wanniarachchi's paper.

2.1.1. Chisholm and Wanniarachchi correlation

This correlation gives the Nusselt number, Nu , as a function of the Reynolds and Prandtl numbers, and the chevron angle of the plates (β), being expressed by

$$Nu = 0.724 \left(\frac{6\beta}{\pi} \right)^{0.646} Re^{0.583} Pr^{1/3}, \quad (2)$$

where the Nusselt number is calculated with the hydraulic diameter, D_h , $Nu = D_h h/k$ [25,26,1].

Eq. (2), agrees with the experimental data of Focke et al. [27] within 15% and 20%, for $\pi/6 \leq \beta \leq 4\pi/6$ and $Re > 1000$. However, the correlation is commonly extrapolated for higher values of the Reynolds number.

2.1.2. Kim correlation

This correlation is developed by using experimental data from a water-to-water plate heat exchanger in single-phase conditions [28]. It also utilises the hydraulic diameter to calculate the Nusselt number as a function of the Reynolds number, Prandtl number, and chevron angle

$$Nu = 0.295 Re^{0.64} Pr^{0.32} \left(\frac{\pi}{2} - \beta \right)^{0.09}. \quad (3)$$

It is quite similar to the aforementioned correlation proposed by Chisholm and Wanniarachchi.

2.1.3. Wanniarachchi correlation

Wanniarachchi et al. also investigated the influence of the chevron angle on the heat transfer coefficient in the case of plate heat exchangers [19]. Unlike the correlations mentioned above, they correlated the data with an asymptotic correlation with two parts, laminar and turbulent. According to them, this correlation satisfies all the three flow regions, including the transition region. It is given by

$$Nu = j_{Nu} Pr^{1/3} (\eta/\eta_w)^{0.17}, \quad (4)$$

$$Nu = \left[\begin{array}{l} (0.2668 - 0.0006967 \times 180\beta/\pi + 7.244 \times 10^5 (180\beta/\pi)^2) \\ (20.7803 - 50.9372\phi + 41.1585\phi^2 - 10.1507\phi^3) \\ Re^{[0.728+0.0543\sin(4\beta+3.7)]} Pr^{1/3} \left(\frac{\eta}{\eta_w} \right)^{0.14} \end{array} \right] \text{ for } \left[\begin{array}{l} \pi/6 \leq \beta \leq \pi/3 \\ Re \geq 1000 \end{array} \right]. \quad (8)$$

where j_{Nu} is the asymptotic value calculated as

$$j_{Nu} = \sqrt[3]{j_{Nu,l}^3 + j_{Nu,t}^3}, \quad (5)$$

where $j_{Nu,l} = 3.65/(90 - 180\beta/\pi)^{0.445} Re^{0.339}$ and $j_{Nu,t} = (12.6/(90 - 180\beta/\pi)^{1.142}) Re^{[0.646+0.00111(90-180\beta/\pi)]}$.

An exponent of 3 is chosen to achieve an asymptotic variation between the laminar and turbulent region [19]. It is suggested that it is used as a preliminary design tool, since

more reliable experimental data are needed to obtain a firm exponent.

2.1.4. Bogaert and Böls correlation

Bogaert and Böls experimentally investigated heat transfer coefficient and pressure drop in some plate heat exchangers [23]. The fact that the Prandtl number and the viscosity ratio exponents are not constant is quite interesting. They depend, respectively, on the Prandtl and Reynolds number

$$Nu = B_1 Re^{B_2} Pr^{\frac{1}{3}} e^{\left(\frac{6.4}{Pr+30} \right)} \left(\frac{\eta}{\eta_w} \right)^{\frac{0.3}{(Re+6)^{0.125}}}, \quad (6)$$

B_1 and B_2 being specific empirical constants which are defined for certain plates and a Reynolds number range as follows

$$\begin{aligned} 0 \leq Re < 20, & B_1 = 0.4621, B_2 = 0.4621 \\ Re = 20, & B_1 = 1.730, B_2 = 0 \\ 20 < Re < 50, & B_1 = 0.0875, B_2 = 1 \\ Re = 50, & B_1 = 4.4, B_2 = 0 \\ 50 < Re < 80, & B_1 = 0.4223, B_2 = 0.6012 \\ Re = 80, & B_1 = 5.95, B_2 = 0 \\ 80 < Re, & B_1 = 0.26347, B_2 = 0.7152 \end{aligned}$$

2.1.5. Muley correlation

This correlation [14,15,20] is quite similar to that proposed by Bogaert and Böls [23]. Unlike this, Muley developed empirical expressions for the parameters B_1 and B_2 in Eq. (6), which are functions of both the chevron angle and the area enlargement factor. The Nusselt number is defined for two ranges of the Reynolds number, and it is valid for a specific range of chevron angles

$$Nu = 0.44 \left(\frac{6\beta}{\pi} \right)^{0.38} Re^{0.5} Pr^{\frac{1}{3}} \left(\frac{\eta}{\eta_w} \right)^{0.14} \text{ for } \left[\begin{array}{l} \pi/6 \leq \beta \leq \pi/3 \\ 30 \leq Re \leq 400 \end{array} \right], \quad (7)$$

and for higher Reynolds numbers,

No correlation was given for Reynolds numbers between 400 and 1000. In this paper, Eq. (8) has been used for $Re \geq 400$, a chevron angle of $\beta = \pi/6$, and an enlargement factor (ϕ) equal to 1.17 (the value commonly used for this type of plate heat exchanger).

2.1.6. Martin correlation

Martin developed a semi-theoretical correlation for the heat transfer coefficient and the pressure drop in plate heat

exchangers [24]. The hydraulic diameter for the Reynolds and Nusselt numbers definition is as mentioned above. The correlation is developed by extending the Leveque theory into the turbulent region, thus

$$Re_h = \phi Re,$$

$$Nu_h = \phi Nu,$$

in a way that the Nusselt number is given as

$$Nu_h = 0.122 Pr^{1/3} \left(\frac{\eta_m}{\eta_w} \right)^{1/6} (f Re^2 \sin 2\beta)^{0.374}, \quad (9)$$

where f is the friction factor which is defined using the distance between the ports of the plate heat exchangers and is given by the following correlation

$$\frac{1}{\sqrt{f}} = \frac{\cos \beta}{(0.18 \tan \beta + 0.36 \sin \beta + f_0/\cos \beta)^{1/2}} + \frac{1 - \cos \beta}{\sqrt{3.8f_1}}, \quad (10)$$

where f_0 and f_1 are defined as in [21,22,24], and are functions of the range of the Reynolds number as

$$Re_h < 2000 \Rightarrow \begin{cases} f_0 = \frac{64}{Re_h} \\ f_1 = \frac{597}{Re_h} + 3.85 \end{cases} \quad (11)$$

$$Re_h \geq 2000 \Rightarrow \begin{cases} f_0 = (1.8 \log_{10} Re_h - 1.5)^{-2} \\ f_1 = \frac{39}{Re_h^{0.289}} \end{cases}$$

The range of validity of the Martin correlation for the Nusselt number is not explicitly given in the original reference. According to Claesson, who varied the Reynolds number between 400 and 10,000, this correlation has a wider applicability due to the possibility of adjusting to experimental data [22].

To illustrate the previous definitions, Fig. 1 compares the correlations introduced above. The Gnielinski correlation [29], which is commonly used for the heat transfer coefficient estimation in tubes, has also been depicted for the sake of comparison. The geometry of plate heat

exchangers and the properties of the flow have been kept constant throughout all the calculations. The correlations have been represented in the form of $Nu/Pr^{0.4}(\eta/\eta_w)^{0.1}$ as functions of the Reynolds number, Re . A proprietary correlation developed by the authors has been included for the sake of comparison.

2.2. Boiling

Boiling inside tubes is dominated by two phenomena: convective boiling and nucleate boiling. Although many boiling correlations have been developed for the characterisation of heat transfer and pressure drop in plate heat exchanger, there is no clear agreement on which effect is dominant. It seems to have been accepted that at high heat fluxes or low qualities, nucleate boiling has a larger influence than convective boiling [30–32]. There are some differences for small plate heat exchangers, for example the heat transfer coefficient seems to be independent from the heat flux as the mechanism of nucleate boiling is dominant and gravity effects are less important [33–35]. Otherwise, the heat transfer coefficient, as in the case of tubes, can be formulated by using either superposition or asymptotic models (which include both convective and nucleate boiling effects) or with enhancement models. The latest simply correct a single-phase correlation with an enhancement factor that accounts for the effect of heat transfer, pressure drop of the refrigerant, heat fluxes, saturation pressure, vapour quality, and so forth. Some correlations also regard the influence of geometric parameters as in the case of single-phase. They prove that variables such as the chevron angle, the pitch, and the hydraulic diameter should not be forgotten in the correlations [16,34]. Models considering the flow pattern are not usual, Gradeck and Lebouché showed that at low gas fluxes two main patterns may be encountered, i.e. stratified at low liquid fluxes and bubbly at high liquid fluxes [6]. Other papers [36] have contributed to a better understanding of the boiling heat transfer coefficient for three different refrigerants: R-134a, R-407C, and R-410A. Some of these correlations are studied in what follows.

2.2.1. Yan and Lin correlation

Yan and Lin investigated flow boiling of R-134a in a single channel plate heat exchanger and reported a correlation for the local heat transfer coefficients [37]. Their results indicate that the evaporation heat transfer coefficient of R-134a in plate heat exchangers is quite different from that in circular pipes, particularly in the convection dominated regime at high vapour qualities. Specifically, at a vapour quality higher than 0.45, the heat transfer coefficient increases almost exponentially with the quality. In accordance with their data, the heat transfer coefficient can be expressed as

$$\left(\frac{\alpha_{tp} D_h}{\lambda_f} \right) Pr_f^{-1/3} Re^{0.5} Bo_{eq}^{-0.3} = 1.926 Re_{eq}, \quad (12)$$

which is valid for a Reynolds range of $2000 < Re_{eq} < 10,000$.

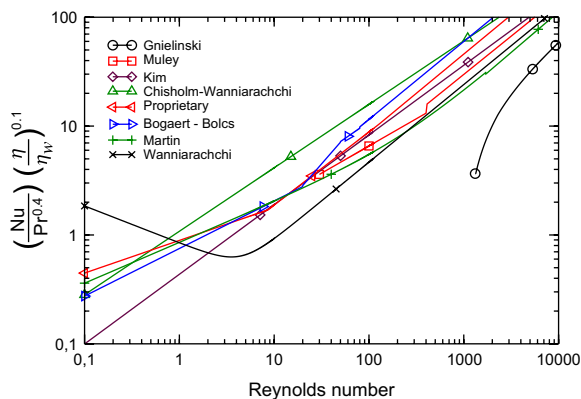


Fig. 1. Nusselt number versus Reynolds number.

In this correlation, Re_{eq} and Bo_{eq} are respectively the equivalent Reynolds and boiling numbers, in which an equivalent mass flux is used in their definitions

$$Re_{eq} = \frac{G_{eq} D_h}{\eta_f},$$

$$Bo_{eq} = \frac{q''_w}{G_{eq} i_{fg}},$$

$$G_{eq} = G \left[1 - x + x \left(\frac{\rho_f}{\rho_g} \right)^{1/2} \right].$$

Heat transfer correlation can be expressed with the Nusselt number of the refrigerant as

$$Nu_r = 1.926 Pr_f^{1/3} Bo_{eq}^{-0.3} Re_{eq}^{0.5} \left[(1-x) + \left(\frac{\rho_f}{\rho_g} \right)^{0.5} \right] \quad \text{for } 2000 < Re_{eq} < 10000. \quad (13)$$

They show, in this case, that at low heat fluxes the heat transfer coefficient depends on vapour quality, contrary to what Han, Lee, and Kim observed for R-410A at high fluxes. They do not show any important influence of heat flux and saturation pressure on the heat transfer coefficient, stating that at low heat fluxes (11 kW/m²) boiling is largely suppressed. After its publication, this correlation was modified considering Webb and Paek's suggestion [38] in such a way that

$$\alpha_r = \begin{cases} 4.36 \frac{\lambda_f}{D_h} Pr_f^{1/3} (1-x)^{-0.5} (C_1 Re_{eq} + C_2) (C_3 Bo + C_4), & \text{if } x \leq 0.7 \\ 4.36 \frac{\lambda_f}{D_h} Pr_f^{1/3} (1-x)^{-0.5} (C_1 Re_{eq} + C_2), & \text{otherwise} \end{cases}, \quad (14)$$

where $C_1 = -0.0124G^{-0.368}$, $C_2 = 1.49G^{0.514}$, $C_3 = -1166x + 1028$, and $C_4 = 0.53e^{0.931x}$.

Thus, the effect of heat flux is neglected at vapour qualities above $x = 0.7$ [39]. In the work carried out in this paper, the original expression (Eq. (13)) has been used, multiplied by a factor of 8 after adjusting it to the experimental results obtained. However, the results obtained with Eq. (14) are not satisfactory at all.

2.2.2. Hsieh and Lin correlation

The correlation proposed by Hsieh and Lin is based on the experimental data obtained for R-410A [40]. The experiments were performed for several mass flow rates, heat fluxes, and system pressures in a heat exchanger characterised by a chevron angle of $\pi/3$

$$\alpha_{r,sat} = \alpha_{r,l} 88 Bo^{0.5},$$

where the all-liquid non-boiling heat transfer coefficient, $\alpha_{r,l}$, is determined from an empirical correlation proposed for R-410A

$$\alpha_{r,l} = 0.2092 \left(\frac{\lambda_f}{D_h} \right) Re^{0.78} Pr^{1/3} \left(\frac{\eta_m}{\eta_w} \right)^{0.14},$$

and the boiling number by $Bo = q/Gi_{fg}$.

They observed that the effect of mass flow rate is negligible on the heat transfer coefficient. However, it is slightly affected by changes in saturation pressure and increases almost linearly with heat flux.

2.2.3. Han, Lee, and Kim correlation

Han–Lee–Kim developed a correlation based on experiments with refrigerants R-22 and R-410A. They varied the mass flow rate of refrigerant, the evaporating temperature, the vapour quality, and the heat flux [34]. Several chevron angles and pitches were also studied. In this case, the Nusselt number is given by

$$Nu = Ge_1 Re^{Ge_2} Bo_{eq}^{0.3} Pr^{0.4},$$

where the coefficients Ge_1 and Ge_2 are functions of the heat exchanger geometry, unlike the Hsieh–Lin correlation presented above

$$Ge_1 = 2.81 \left(\frac{p_{co}}{D_h} \right)^{-0.041} \left(\frac{\pi}{2} - \beta \right)^{-2.83},$$

$$Ge_2 = 0.746 \left(\frac{p_{co}}{D_h} \right)^{-0.082} \left(\frac{\pi}{2} - \beta \right)^{0.61},$$

where Bo_{eq} and Re_{eq} are defined as before. They also show a slight increase of the heat transfer coefficient with the mass flow rate which is higher for low chevron angles. Furthermore, they show that the heat transfer coefficient decreases with temperature and only increases a little with vapour quality. Heat flux has almost no effect, as only at low heat fluxes certain increases of the coefficient are reported. It should be noticed that the values of the heat fluxes are much lower than those used by Hsieh and Lin [40].

2.2.4. Adapted Thonon correlation and asymptotic correlation

The authors propose two different correlations. The first one is inspired by that proposed by Thonon et al. in [41,32]. Unlike Thonon's paper, the maximum value between the nucleate and the convective boiling contributions is chosen as the heat transfer coefficient

$$\alpha_r = \max\{\alpha_{nb}, \alpha_{cb}\}. \quad (15)$$

Thonon originally used the product of the boiling and the Lockhart–Martinelli parameters (BoX_{tt}) as criterion for the transition between nucleate boiling and convective evaporation.

The second one is an asymptotic model with the exponent $n = 2$, as suggested by Kutateladze [42], such that the heat transfer coefficient is given by

$$\alpha_r = \{ \alpha_{nb}^2 + \alpha_{cb}^2 \}^{1/2}, \tag{16}$$

which uses, as in the previous case, the following nucleate and convective boiling coefficients

$$\alpha_{cb} = F\alpha_f,$$

$$\alpha_{nb} = S\alpha_{pb},$$

$$F = \left(a_1 + \frac{a_2}{X_{tt}} \right)^{a_3},$$

$$S = (1 + a_4 Re_f F)^{-1}.$$

The single-phase correlation used in the convective contribution is a suitable equation adjusted for plate heat exchangers (e.g. Bogaert and Bölcs). In the case of the nucleate boiling contribution, the Cooper correlation has been used [43]. The parameters in the enhancement and suppression factors can be obtained by correlating them with experimental results.

The heat transfer coefficient correlations presented above have been compared in Figs. 2 and 3. The values gathered in these figures correspond to the coefficients as a function of the vapour quality for several mass flow rates (15, 30 and 60 kg/m²s) and heat fluxes (5000, 10,000 and 15,000 W/m²), covering a wide range of practical cases. The evaporation pressure considered in the calculations is $p = 5$ bar, the hydraulic diameter is $D_h = 3.5 \times 10^{-3}$ m, and the refrigerant studied is R-410A. During the numerical calculations, the ranges for these representations have been chosen by taking into account the values that these variables have. From the figures, the low influence of the mass flow rate in correlations such as Han–Lee–Kim and Hsieh–Lin can be observed. Similarly, the heat flux has a slight effect on the values provided by the Han–Lee–Kim correlation. This influence is more important in other correlations, mostly in the adapted Thonon correlation and the asymptotic correlation.

2.3. Condensation

Two main phenomena affecting the flow pattern in condensation are gravity and shear stress and these make some difference in the way correlations are developed. As in the evaporation case, there are correlations based on enhancing single-phase correlations by means of a multiplier. In this way, the condensation heat transfer coefficient is correlated as a function of the Reynolds and the Prandtl numbers through an expression of the form

$$Nu = AR e^b Pr_f^c, \tag{17}$$

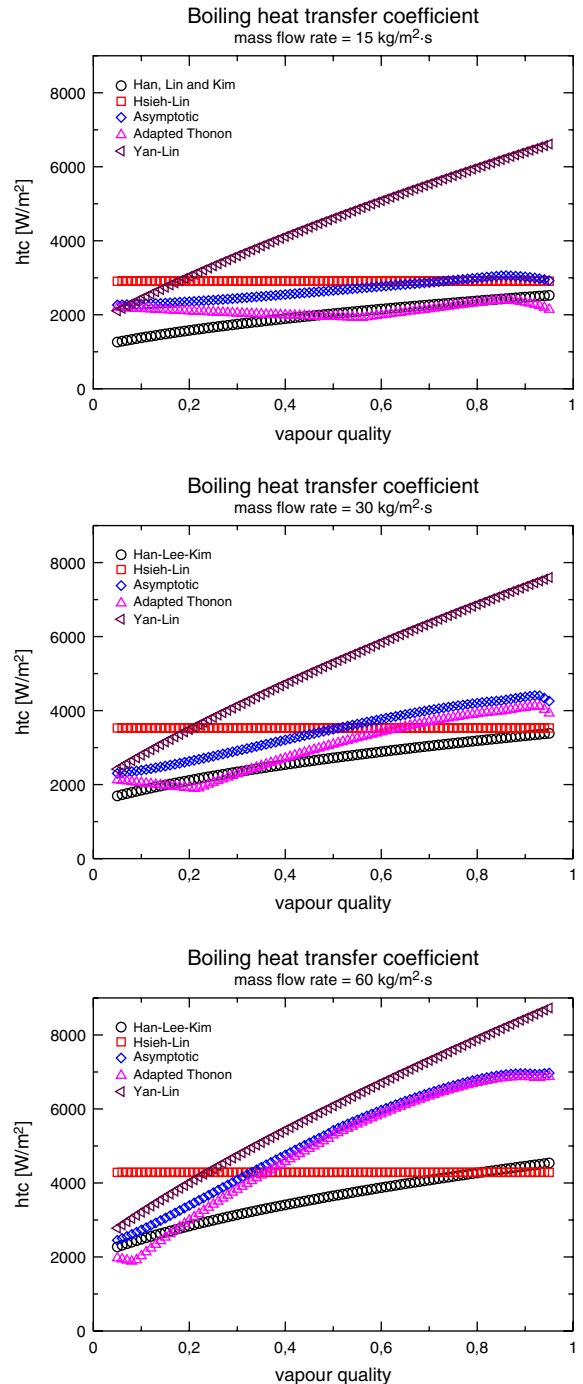


Fig. 2. Heat transfer coefficient at different mass flow rates (15, 30 and 60 kg/m²s) and constant heat flux $q = 6000$ W/m².

where A , b and c are correlated with experimental data. Some correlations can be highlighted: Thonon and Bontemps’s work on hydrocarbons [44]; Yan et al. on R-134a [45]; or Würfel and Ostrowski’s work which studies

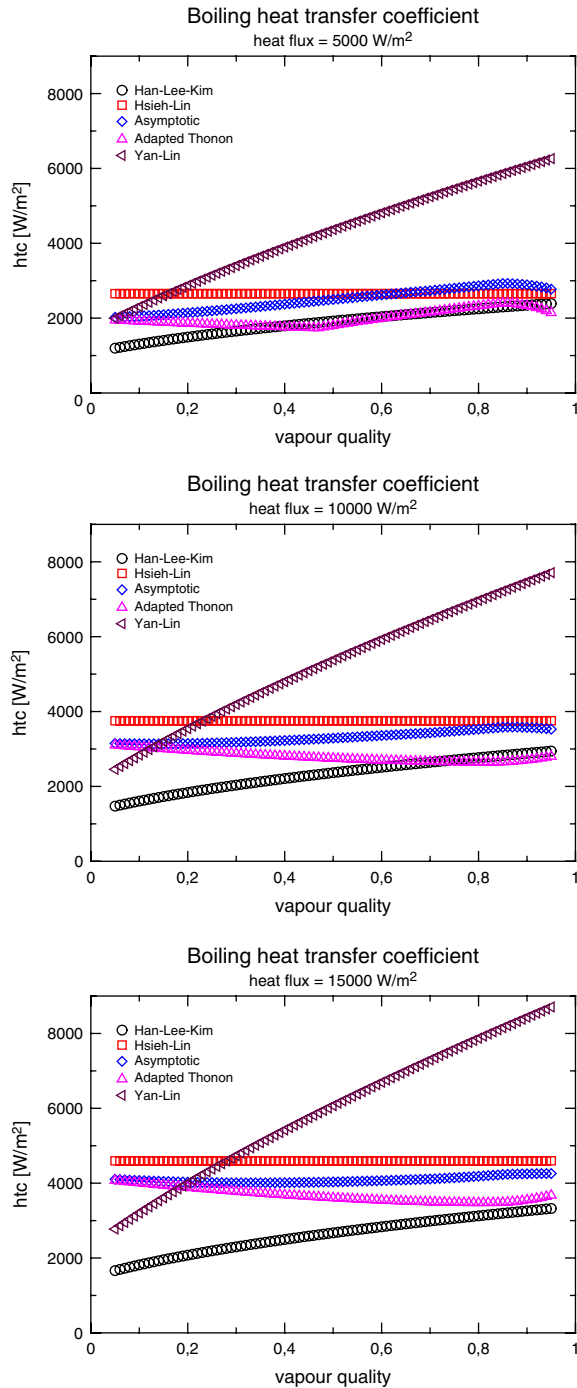


Fig. 3. Heat transfer coefficient at different heat fluxes (5000, 10,000 and 15,000 W/m²) and constant mass flow rate $m = 15 \text{ kg/m}^2\text{s}$.

the condensation of *n*-heptane and the influence of different plates combinations [46].

In other cases, it is proposed that the Reynolds number be evaluated by using an equivalent mass flow rate,

$G_{eq} = G[1 - x + x(\rho_f/\rho_g)^{1/2}]$, which takes into account the effect of the mass flux, the vapour quality, and the condensation pressure. Furthermore, other correlations include the effects of the heat flux [47] or the effect of the chevron angle [48] by introducing the boiling number or the angle in the expressions, respectively.

2.3.1. Yan, Lio, and Lin correlation

Yan–Lio–Lin studied the condensation heat transfer coefficient and the friction pressure drop of R-134a in vertical plate heat exchangers [45]. They studied the influence of mass flux, heat flux, system pressure, and vapour quality for a chevron angle of 60°. They suggested the following correlation for the condensation heat transfer coefficient

$$\alpha_r = 4.118 \left(\frac{\lambda_f}{D_h} \right) Re_{eq}^{0.4} Pr_f^{1/3}, \tag{18}$$

where $Re_{eq} = (G_{eq}D_h/\eta_f)$, and $G_{eq} = G[1 - x + x(\rho_f/\rho_g)^{1/2}]$.

The condensation heat transfer coefficient increases slightly with the mass flow rate and the heat flux, with the effect of the heat flux being less important. It decreases as the refrigerant is condensing. Some abrupt changes in the heat transfer coefficient have been reported at certain vapour qualities ($x \approx 0.6$), they were explained by a change from turbulent to laminar flow due to a smaller vapour flow rate as it disappears. However, increasing condensation pressure makes the heat transfer increase.

2.3.2. Shah-modified-correlation

This correlation is a modified version of that proposed by Shah for film condensation inside tubes [49]. In the original formulation, the heat transfer coefficient is equal to the liquid heat transfer coefficient enhanced by means of a multiplier, in this case, the correlation proposed is

$$\alpha = c_1 Re_f^{c_2} Pr_f^{c_3} \frac{\lambda_f}{D_h} \left((1-x)^{d_1} + \frac{3.8x^{d_2}(1-x)^{0.04}}{p^{0.38}} \right). \tag{19}$$

The differences between this correlation and that initially proposed by Shah are in the parameters of the single-phase heat transfer coefficient c_1 , c_2 , and c_3 and the enhancement factor parameters d_1 and d_2 . These can be adjusted by considering a convenient experimental database.

2.3.3. Kuo, Lie, Hsieh, and Lin correlation

This correlation has been developed by using experimental data on R-410A in vertical plate heat exchangers [50,47]. The heat transfer coefficient is given by

$$\alpha_{tp} = \alpha_f [0.25Co^{-0.45}Fr_f^{0.25} + 75Bo^{0.75}],$$

where $\alpha_f = 0.2092(\lambda_f/D_h)Re_f^{0.78}Pr_f^{1/3}(\eta_{tm}/\eta_{fw})^{0.14}$, $Co = (\rho_g/\rho_f)(1-x/x)^{0.8}$, $Fr_f = G^2/\rho_f^2gD_h$, $Bo = q/Gi_{fg}$, $Re_{eq} = G_{eq}D_h/\eta_f$, and the equivalent mass flow rate has the same definition as above, $G_{eq} = G(1 - x + x(\rho_f/\rho_g)^{0.5})$.

The heat transfer coefficient increases when the mass flow rate and the heat flux increase. In the case of mass flow, the effect is greater at higher vapour qualities and it is lower at low qualities than at high qualities. The abrupt change in the coefficient, noticed for R-134 at a certain vapour quality, is not found for R-410A. The effect of pressure on the heat transfer coefficient is negligible, as happens for R-134a in the above correlation. This coefficient is slightly influenced by heat flux, increasing somewhat with it. It also increases with mass flow rate and presents larger values at low vapour qualities. This effect is higher as the fluid condenses.

2.3.4. Han, Lee, and Kim correlation

They proposed a similar correlation to that which they had proposed for evaporation in plate heat exchangers [48].

The refrigerants used in the experiments were R-22 and R-410A and they varied the mass flux, the condensation temperature and the vapour quality. This was done for chevron angles of 45°, 35°, and 20°. Again, the proposed heat transfer coefficient has the form

$$Nu = Ge_1 Re_{eq}^{Ge_2} Pr^{1/3},$$

where the coefficients Ge_1 and Ge_2 are functions of the heat exchanger geometry, unlike the condensation correlations presented above. In this case, the expressions of the coefficients Ge_1 and Ge_2 are

$$Ge_1 = 11.22 \left(\frac{p_{co}}{D_h} \right)^{-2.83} \left(\frac{\pi}{2} - \beta \right)^{-4.5},$$

$$Ge_2 = 0.35 \left(\frac{p_{co}}{D_h} \right)^{0.23} \left(\frac{\pi}{2} - \beta \right)^{1.48},$$

They show that the heat transfer coefficient is slightly affected by the mass flow rate and the condensation temperature. When the chevron angle is smaller, the effect is larger. On the other hand, the coefficient decreases as the refrigerant condenses (decreasing vapour qualities). In this case, the heat fluxes are not as big as in previous correlations.

2.3.5. Thonon correlation

Thonon and Bontemps proposed a correlation for the heat transfer coefficient for pure hydrocarbons (pentane, butane, and propane) and mixtures of hydrocarbons (butane + propane) [44]. They studied operation pressures from 1.5 to 1.8 bar, identifying two different condensation mechanisms or effects for pure fluids. At low Reynolds numbers, condensation is almost filmwise and the heat transfer coefficient decreases with increasing Reynolds number. This is contrary to what happens at high Reynolds numbers, in which case the coefficient increases slightly. The correlation proposed for pure fluids is

$$\alpha = \alpha_{i0} 1564 Re_{eq}^{-0.76}. \tag{20}$$

where Re_{eq} is evaluated as in previous sections. They checked that the three hydrocarbon fluids have a similar behaviour as their physical properties are quite similar.

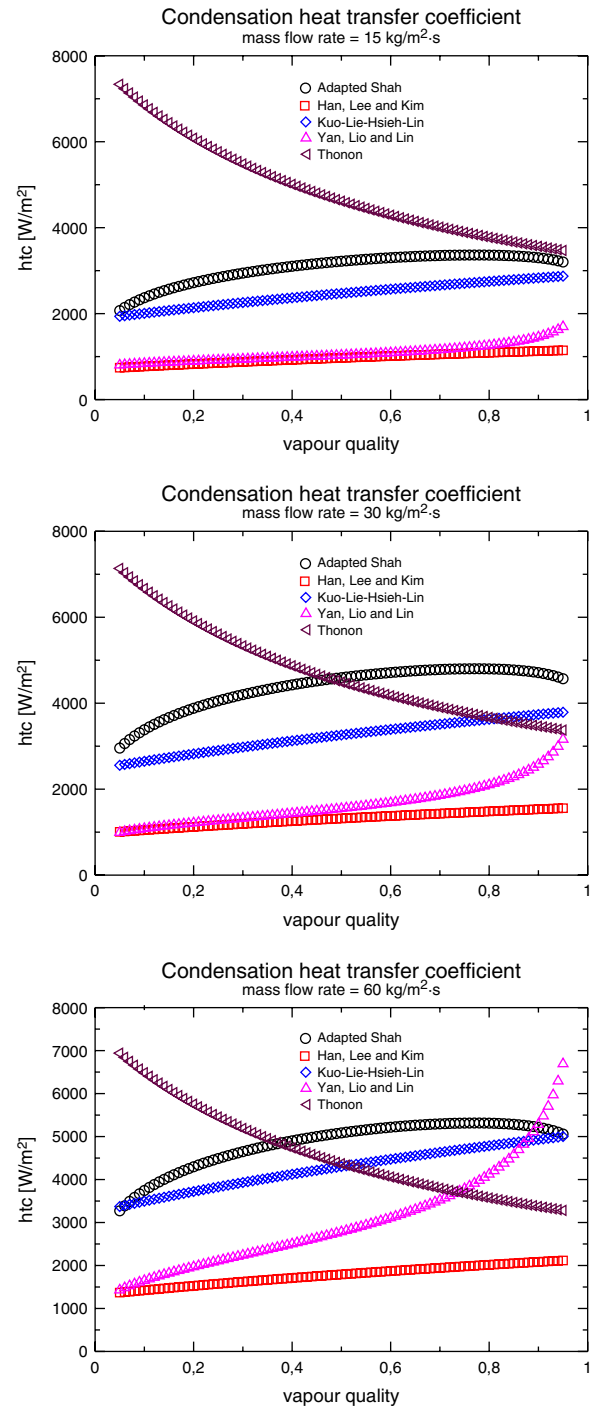


Fig. 4. Heat transfer coefficient at different mass flow rates (15, 30 and 60 kg/m²·s) and constant heat flux $q = 6,000 \text{ W/m}^2$.

The heat transfer coefficient correlations presented above are compared in Figs. 4 and 5. They vary with the vapour quality at several mass flow rates (15, 30 and 60 kg/m²s) and heat fluxes (5000, 10,000 and 15,000 W/m²), covering a wide range of practical cases. They correspond to the values encountered in the calculations carried out throughout this study. The evaporation pressure considered in the calculations is $p = 20$ bar, the hydraulic diameter is $D_h = 3.5 \times 10^{-3}$ m, and the refrigerant studied is R-410A.

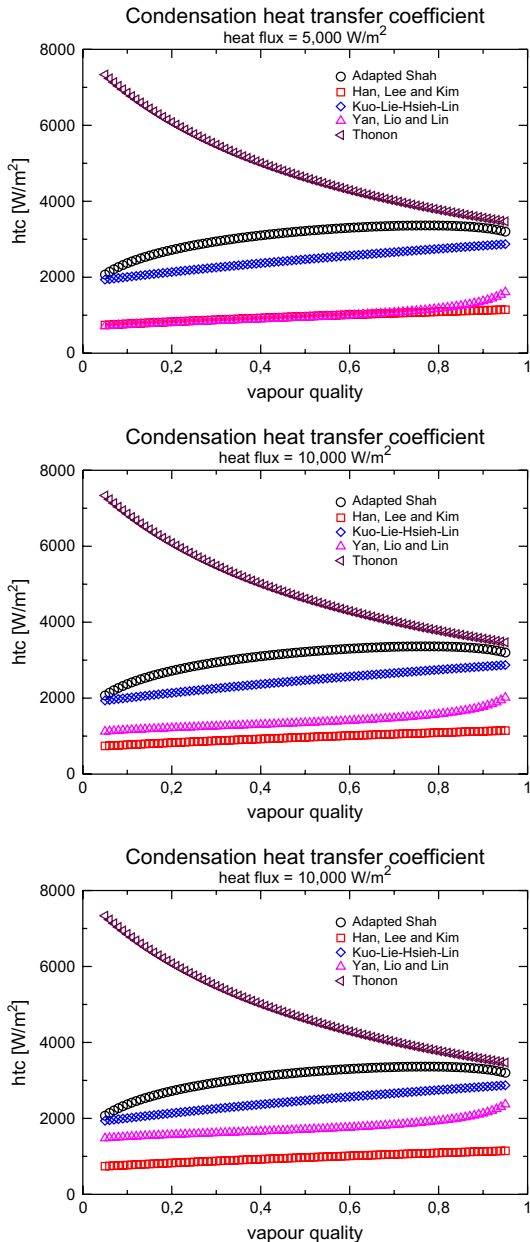


Fig. 5. Heat transfer coefficient at different heat fluxes (5000, 10,000 and 15,000 W/m²) and constant mass flow rate $m = 15$ kg/m²s.

The adapted Shah and Kuo–Lie–Hsieh–Lin correlations are more influenced by mass flow rate changes than the others. The Yan–Lio–Lin correlation provides high values for the heat transfer coefficient at high mass flow rates, when the vapour quality approaches 1. A different trend is observed in the Thonon correlation where the heat transfer coefficient increases as the fluid condenses and the vapour quality has values nearer to 0.

3. Experimental results versus calculated results

Several measurements were carried out, some of them with R-22 and others with R-290. Furthermore, two plate heat exchangers have been studied: one with 38 plates and another with 46 plates. Both of them have L passages and a pitch of 2.35 mm. They worked in counter-current mode in the condensation case and in co-current mode in the evaporation case. From the different data compiled during the data acquisition campaign, this analysis only considers the evaporation and condensation temperatures.

3.1. Boiling case

The experimental tests have been run following the modelling procedure described in [2] and using the previously mentioned ART[®] code. The results obtained have been produced utilising the correlations presented above namely Han–Lee–Kim, Hsieh–Lin, Yan–Lin, Cooper, and two adapted versions for plate heat exchangers (the Thonon correlation [32,41] and an asymptotic correlation [51]). The comparison between the experimental results and the calculated values for these correlations is displayed in Figs. 6–8. Lines corresponding to ± 2 °C have been depicted simply for the sake of clarity. Good agreement is encountered between the experimental and the computational results. It is remarkable that a correlation such as the Cooper correlation provides such good results. This shows that nucleate boiling

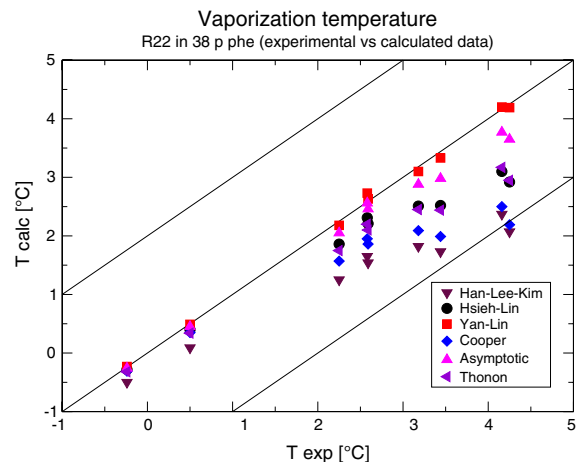


Fig. 6. Experimental results versus numerical results.

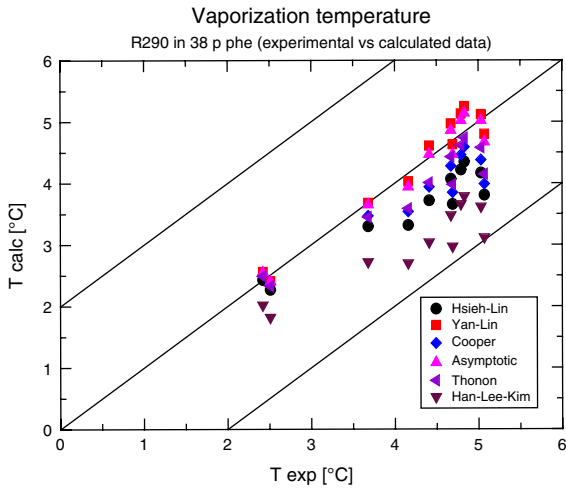


Fig. 7. Experimental results versus numerical results.

plays an important role, at least under the conditions in which the experiments have been performed.

3.2. Condensation case

Similarly to what has been done in the previous study with the evaporation temperature, the condensation temperature is the variable examined to assess the agreement between the condensation correlations and the experimental data. The methodology applied to model the experiments is the same as that introduced in [3]. As in that case, the model does not consider wet wall conditions in the desuperheating region. Its effect in the condensation temperature calculation is also practically negligible. The comparison between the experimental results and the calculated values is displayed in Figs. 9–11. Lines corresponding to $\pm 5^\circ\text{C}$ differences have been depicted for the sake of comparison

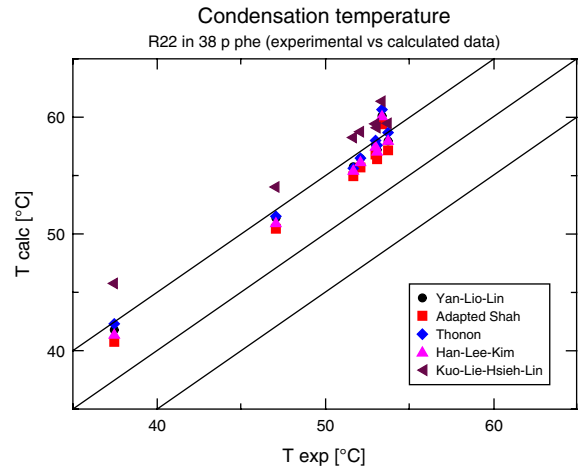


Fig. 9. Experimental results versus numerical results.

and clarity. Good agreement is also observed between the experimental data and most of the calculated values.

4. Conclusions

This paper closes a series of papers that study the behaviour of a model for the characterisation of refrigeration equipments by means of the evaporation or condensation temperature, depending on the case. It focuses on the study of heat transfer in plate heat exchangers, comparing different correlations for the evaluation of the heat transfer coefficient. Previous contributions have already described the model used, the methodology employed in the numerical studies, and the facility used for carrying out the experiments. A description of the heat exchangers employed in the experiment is also included. The correlations studied have been for both evaporation and condensation. They

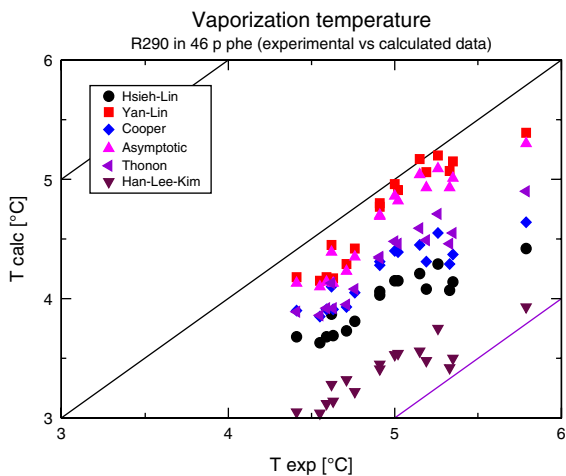


Fig. 8. Experimental results versus numerical results.

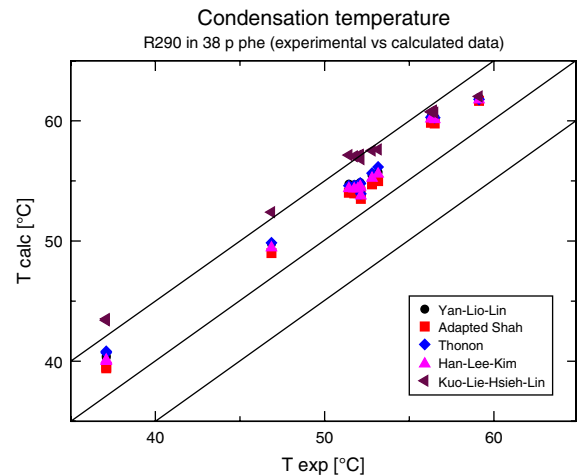


Fig. 10. Experimental results versus numerical results.

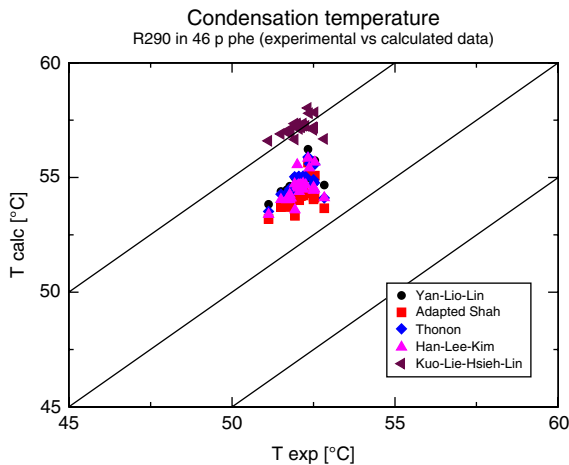


Fig. 11. Experimental results versus numerical results.

have been described in some detail and compared by taking into account the ranges of heat and mass flux studied in the experiments. In the case of evaporation, three well-known correlations have been studied and compared with the Cooper correlation and two correlations traditionally applied to fin and tube heat exchangers have been adapted by the authors to plate heat exchangers. The good results obtained with the Cooper correlation lead to the conclusion that nucleate boiling plays an important role in the test cases studied in this work. As far as the condensation case is concerned, five correlations have been studied and the results obtained make them quite appealing for the analysis and characterisation of the behaviour of this sort of heat exchanger.

Again, the use of the evaporation and condensation temperatures as design parameters has been demonstrated to be a good idea as they are more sensitive to misleading variations of the heat transfer coefficient than other parameters such as the COP or the refrigeration and the heating capacities. It should be pointed out that the correlations described in this paper have been applied to model particular plate heat exchangers working with R-22 and R-290, although many of them have been developed for different refrigerants, geometries, and flow conditions.

Acknowledgements

This research has been partially financed by the following bodies: Fundación Séneca (CARM), project 00693/PPC/04 and Ministerio de Educación y Ciencia (MEC), project DPI2005-09262-C02-02.

The authors would like to acknowledge the experimental work carried out by Javier Blanco at the Universidad Politécnica de Valencia.

The authors also wish to thank Ms Juana Mari Belchí and Ms Neasa Conroy for assistance with the English translation.

References

- [1] R.K. Shah, A.S. Wanniarachchi, Plate Heat Exchanger Design Theory, von Karman Institute of Fluid Dynamics, 1991.
- [2] J.R. García-Cascales, F. Vera-García, J.M. Corberán-Salvador, J. González-Maciá, D. Fuentes-Díaz, Assessment of boiling heat transfer correlations in the modelling of tube and fin heat exchangers. *International Journal of Refrigeration*, in press. doi:10.1016/j.ijrefrig.2007.01.006.
- [3] F. Vera-García, J.R. García-Cascales, J.M. Corberán-Salvador, J. González-Maciá, D. Fuentes-Díaz, Assessment of condensation heat transfer correlations in the modelling of fin and heat exchangers. *International Journal of Refrigeration*, in press. doi:10.1016/j.ijrefrig.2007.01.005.
- [4] J.M. Corberán, P. Fernández de Córdoba, J. González, F. Alias, Semiexplicit method for wall temperature linked equations (SEWTLE): a general finite-volume technique for the calculation of complex heat exchangers, *Numerical Heat Transfer (2000)* 37–59.
- [5] J.M. Corberán, J. González, P. Montes, R. Blasco, 'ART' a computer code to assist the design of refrigeration and A/C equipment, in: *Ninth International Refrigeration and Air Conditioning Conference*, Purdue, 2002.
- [6] M. Gradeck, M. Lebouché, Two-phase gas-liquid flow in horizontal corrugated channels, *International Journal of Multiphase Flow* 26 (2000) 435–443.
- [7] G. Kreissing, H.M. Müller-Steinhagen, Frictional pressure drop for gas/liquid two-phase flow in plate heat exchangers, *Heat Transfer Engineering* 13 (1992) 42–52.
- [8] C. Tribbe, H.M. Müller-Steinhagen, Gas/liquid flow in plate-and-frame heat exchangers-part i: pressure drop measurements, *Heat Transfer Engineering* 22 (2001) 5–11.
- [9] C. Tribbe, H.M. Müller-Steinhagen, Gas/liquid flow in plate-and-frame heat exchangers-part ii: two-phase multiplier and flow pattern analysis, *Heat Transfer Engineering* 22 (2001) 12–21.
- [10] P. Vlasogiannis, G. Karagiannis, P. Argyropoulos, V. Bontozoglou, Air-water two-phase flow and heat transfer in a plate heat exchanger, *International Journal of Multiphase Flow* 28 (2002) 757–772.
- [11] Y.Y. Hsieh, L.J. Chiang, T.F. Lin, Subcooled flow boiling heat transfer of R134a and the associated bubble characteristics in a vertical plate heat exchanger, *International Journal of Heat and Mass Transfer* 45 (2002) 1792–1806.
- [12] G.A. Longo, A. Gasparella, R. Sartori, Experimental heat transfer coefficient during refrigerant vaporisation and condensation inside herringbone-type plate heat exchangers with enhanced surfaces, *International Journal of Heat and Mass Transfer* 47 (2004) 4124–4136.
- [13] R.A. Troupe, J.C. Morgan, J. Priffiti, The plate heater versatile chemical engineering tool, *Chemical Engineering Progress* 56 (1960) 124–128.
- [14] A. Muley, R.M. Manglik, Experimental study of turbulent flow heat transfer and pressure drop in a plate heat exchanger with chevron plates, *Journal of Heat Transfer, ASME* 121 (1999) 110–117.
- [15] A. Muley, R.M. Manglik, H.M. Metwally, Enhanced heat transfer characteristics of viscous liquid flows in a chevron plate heat exchanger, *Journal of Heat Transfer, ASME* 121 (1999) 1011–1017.

- [16] Z.H. Ayub, Plate heat exchanger literature survey and new heat transfer and pressure drop correlations for refrigerant evaporators, *Heat Transfer Engineering* 24 (2003) 3–16.
- [17] H. Kumar, The plate heat exchanger: construction and design, Institute of Chemical Engineering Symposium Series 86 (1984) 1275–1288.
- [18] R.L. Heavner, H. Kumar, A.S. Wanniarachchi, Performance of an industrial heat exchanger: effect of chevron angle, in: *AIChE Symposium Series*, vol. 89, AIChE, New York, 1993, pp. 262–267.
- [19] A.S. Wanniarachchi, U. Ratnam, B.E. Tilton, K. Dutta-Roy, Approximate correlations for chevron-type plate heat exchangers, in: *Proceedings of the 30th National Heat Transfer Conference*, vol. 12, HTD, ASME-vol. 314, New York, 1995, pp. 145–151.
- [20] A. Muley, Heat Transfer and Pressure Drop in Plate Heat Exchangers, Ph.D. thesis, Dept. Mechanical, Industrial and Nuclear Engineering, Div. Graduate Studies and Research, University of Cincinnati, UNI Number: 9804592, 1997.
- [21] J. Claesson, Thermal and hydraulic characteristic of brazed plate heat exchangers-part i: review of single-phase and two-phase adiabatic and flow boiling characteristics, in: *ASHRAE Transactions Symposia*, 2005.
- [22] J. Claesson, Thermal and Hydraulic Performance of Compact Brazed Plate Heat Exchangers Operating as Evaporators in Domestic Heat Pumps, Ph.D. thesis, KTH Energy Technology, 2004.
- [23] R. Bogaert, A. Bölcs, Global performance of a prototype brazed plate heat exchanger in a large Reynolds number range, *Experimental Heat Transfer* 8 (1995) 293–311.
- [24] H. Martin, A theoretical approach to predict the performance of chevron-type plate heat exchangers, *Chemical Engineering Process* 35 (1996) 301–310.
- [25] D. Chisholm, A.S. Wanniarachchi, Plate heat exchangers: plate selection and arrangement, in: *Presented at AIChE Meeting*, Orlando, Florida, March 18–22, 1990.
- [26] D. Chisholm, A.S. Wanniarachchi, Layout of plate heat exchangers, in: *ASME/JSME Thermal Engineering Proceedings*, vol. 4, ASME, New York, 1991, pp. 433–438.
- [27] W.W. Focke, J. Zachariades, I. Oliver, The effect of the corrugation inclination angle on the thermohydraulic performance of plate heat exchangers, *International Journal of Heat and Mass Transfer* 28 (1985) 1469–1479.
- [28] Y.S. Kim, An Experimental Study on Evaporation Heat Transfer Characteristics and Pressure Drop in Plate Heat Exchanger, M.S. thesis, Yonsei University, 1999.
- [29] V. Gnielinski, Forced convection in ducts, in: E.U. Schlunder (Ed.), *Heat Exchanger Design Handbook*, Hemisphere Publishing Corp., Washington, DC, 1983 (2, Section 2.5.1).
- [30] Marvillet, Welded plate heat exchangers as refrigerants dry-ex evaporator, in: *Design and Operation of Heat Exchangers*, Springer-Verlag, 1992, pp. 255–268.
- [31] D. Sterner, B. Sundén, Performance of plate heat exchangers for evaporation of ammonia, *Heat Transfer Engineering* 27 (2006) 45–55.
- [32] C.C. Thonon, R. Vidil, C. Marvillet, Recent research and developments in plate heat exchangers, *Journal of Enhanced Heat Transfer* 2 (1995) 149–155.
- [33] J. Claesson, B. Palm, Boiling mechanism in a small compact brazed plate heat exchanger (cbe) determined by using thermochromic liquid crystal (tlc), in: *20th International Congress of Refrigeration, IIR/IIF*, Sydney, 1999.
- [34] D.H. Han, K.J. Lee, Y.H. Kim, Experiments on characteristics of evaporation of R410a in brazed plate heat exchangers with different geometric configurations, *Applied Thermal Engineering* 23 (2003) 1209–1225.
- [35] O. Pelletier, B. Palm, Condensation and boiling of hydrocarbons in small plate heat exchangers, *Nordiske köleogvarmepumpedager*, Reykavik, Island, June 19–22, 1997.
- [36] G. Boccardi, G.P. Celata, M. Cumo, The use of new refrigerants in compact heat exchangers for the refrigeration industry, *Heat Transfer Engineering* 21 (2000) 53–62.
- [37] Y.Y. Yan, T.F. Lin, Evaporation heat transfer and pressure drop of refrigerant R134a in a plate heat exchanger, *Transaction of the ASME, Journal of Heat Transfer* 121 (1999) 118–127.
- [38] R.L. Webb, J.W. Paek, Letter to the editor, *International Journal of Heat and Mass Transfer* 46 (2003) 1111–1112.
- [39] Y.Y. Yan, T.F. Lin, Letter to the editor, *International Journal of Heat and Mass Transfer* 26 (2003) 1112–1113.
- [40] Y.Y. Hsieh, T.F. Lin, Saturated flow boiling heat transfer and pressure drop of refrigerant R410a in a vertical plate heat exchanger, *International Journal of Heat and Mass Transfer* 45 (2002) 1033–1044.
- [41] C.C. Thonon, A. Feldman, L. Margat, C. Marvillet, Transition from nucleate boiling to convective boiling in compact heat exchangers, *International Journal of Refrigeration* 20 (1997) 592–597.
- [42] S.S. Kutateladze, Boiling heat transfer, *International Journal of Heat and Mass Transfer* 4 (1961) 3–45.
- [43] M.G. Cooper, Heat flow rates in saturated nucleate pool boiling, *Advances in Heat Transfer* 16 (1984) 157–239.
- [44] B. Thonon, A. Bontemps, Condensation of pure and mixture of hydrocarbons in a compact heat exchanger: experiments and modelling, *Heat Transfer Engineering* 23 (2002) 3–17.
- [45] Y.Y. Yan, H.C. Lio, T.F. Lin, Condensation heat transfer and pressure drop of refrigerant R134a in a plate heat exchanger, *International Journal of Heat and Mass Transfer* 42 (1999) 993–1006.
- [46] R. Würfel, N. Ostrowski, Experimental investigations of heat transfer and pressure drop during the condensation process within plate heat exchangers of the herringbone type, *International Journal of Thermal Sciences* 43 (2004) 59–68.
- [47] W.S. Kuo, Y.M. Lie, Y.Y. Hsieh, T.F. Lin, Condensation heat transfer and pressure drop of refrigerant R410a flow in a vertical plate heat exchanger, *International Journal of Heat and Mass Transfer* 48 (2005) 5205–5220.
- [48] D.H. Han, K.J. Lee, Y.H. Kim, The characteristics of condensation in brazed plate heat exchangers with different chevron angles, *Journal of the Korean Physical Society* 43 (2003).
- [49] M.M. Shah, A general correlation for heat transfer during film condensation inside pipes, *International Journal of Heat and Mass Transfer* 22 (1979) 547–556.
- [50] Y.Y. Hsieh, Y.M. Lie, T.F. Lin, Condensation heat transfer and pressure drop of refrigerant R-410a in a vertical plate heat exchanger, in: *Third International Symposium on Two-Phase Flow Modelling and Experimentation*, vol. 1, Pisa, Italy, September 22–24, 2004.
- [51] J.C. Chen, A correlation for boiling heat transfer to saturated fluids in convective flow, *Industrial and Engineering Chemistry Process Design and Development* 5 (1966) 322–329.